

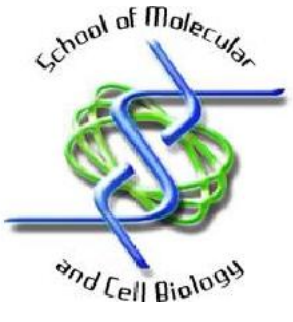
https://dspace.org/

Investigating the epigenetic regulation of manganese superoxide dismutase in aging rat tissue

Bayley, Cassidy

2016-01-20
http://hdl.handle.net/10539/19358

Downloaded from a DSpace repository. https://dspace.org/





Investigating the Epigenetic Regulation of Manganese Superoxide Dismutase in Aging Rat Tissue

By Cassidy Bayley

A Dissertation submitted to the Faculty of Science, University of the Witwatersrand, Johannesburg, in fulfilment of the requirements for the degree of Master of Science.

Supervisor: Dr Natalya Nikitina

Johannesburg, 2015

DECLARATION

I, Cassidy Bayley (364888), am a student registered for the degree of Master of Science in the academic year 2015.

I hereby declare the following:

- I am aware that plagiarism (the use of someone else's work without their permission and/or without acknowledging the original source) is wrong.
- I confirm that the work submitted for assessment for the above degree is my own unaided work except where explicitly indicated otherwise and acknowledged.
- I have not submitted this work before for any other degree or examination at this or any other University.
- The information used in the Dissertation has not been obtained by me while employed by, or working under the aegis of, any person or organisation other than the University.
- I have followed the required conventions in referencing the thoughts and ideas of others.
- I understand that the University of the Witwatersrand may take disciplinary action against me if there is a belief that this is not my own unaided work or that I have failed to acknowledge the source of the ideas or words in my writing.

Signature Bayley **day of** 24/08/ **2015**

DEDICATION

This work is dedicated to my dearly loved grandmother, Nora Bayley, who taught me that one should never stop learning.

ACKNOWLEDGEMENTS

I would like to thank the University of the Witwatersrand as well as the National Research Foundation for their financial support throughout the undertaking of this Dissertation. I would also like to thank my supervisor, Dr Nikitina, for her guidance and support.

RESEARCH OUTPUTS

Conference output:

Poster presentation

By Cassidy Bayley

Investigating the epigenetic regulation of manganese superoxide dismutase in aging rat tissue.

MBRT Research Day, University of the Witwatersrand, 4 December 2014.

TABLE OF CONTENTS

1. LIST OF FIGURES, TABLES AND ABBREVIATIONS 6
   1.1. LIST OF FIGURES 6
   1.2. LIST OF TABLES 8
   1.3. LIST OF ABBREVIATIONS 9
2. ABSTRACT 12
3. INTRODUCTION 13
   3.1. AGING, AGE-RELATED DISEASE AND THE FREE RADICAL THEORY 13
   3.2. ANTIOXIDANT DEFENSES IN AGING, CANCER AND NEURODEGENERATIVE DISEASE 16
   3.3. EPIGENETIC TRENDS IN AGING, CANCER AND NEURODEGENERATIVE DISEASE 18
   3.4. EPIGENETIC REGULATION OF MNSOD IN DISEASE 21
   4. SIGNIFICANCE OF THIS WORK 23
   5. HYPOTHESIS, AIM AND OBJECTIVES 24
   5.1. HYPOTHESIS 24
   5.2. AIM AND OBJECTIVES 24
   6. MATERIALS AND METHODS 25
   6.1. SOD2 PROMOTER ANNOTATION 25
   6.1.1. Basic SOD2 gene annotation 25
   6.1.2. PATCH analysis 25
   6.1.3. Comprehensive SOD2 promoter annotation 25
   6.2. REVERSE TRANSCRIPTION QUANTITATIVE PCR (RT-PCR) 26
   6.2.1. Primer design 26
   6.2.2. RNA extraction 28
   6.2.3. Reverse transcription 29
   6.2.4. Quantitative PCR 29
   6.3. BISULFITE DNA CONVERSION AND METHYLATION-SPECIFIC PCR 34
   6.3.1. Primer design 34
   6.3.2. Genomic DNA extraction 35
   6.3.3. Bisulfite conversion 35
   6.3.4. Methylation-specific PCR 35
   6.3.5. DNA cloning 36

6.3.6. Sequencing and analysis 37

7. RESULTS 38

7.1. GENE ANNOTATION ELUCIDATES THE PUTATIVE TRANSCRIPTIONAL AND EPIGENETIC REGULATORY SITES IN THE RAT SOD2 GENE PROMOTER 38

7.1.1. Basic SOD2 gene annotation illustrating conservation and GC frequency 38

7.1.2. PATCH analysis reveals putative transcriptional binding sites in the SOD2 promoter 39

7.1.3. Comprehensive SOD2 promoter annotation 40

7.2. RT-PCR REVEALS AN INCREASE IN SOD2 EXPRESSION IN AGING LIVER AND A DECREASE IN SOD2 EXPRESSION IN AGING BRAIN 41

7.2.1. Confirmation of extracted RNA quality 41

7.2.2. Melting curve analysis reveals target specificity for all genes 42

7.2.3. Standard curve analysis confirms the efficiency, precision and sensitivity of RT-PCR gene amplification 45

7.2.4. Data normalization reveals a relative increase in SOD2 mRNA levels in aging rat liver and a relative decrease in aging rat brain 48

7.2.5. Statistical analysis reveals that differences in SOD2 mRNA levels in young and old rat tissue are insignificant 50

7.3. A METHYLATION ASSAY REVEALS THAT THE RAT SOD2 PROMOTER REMAINS LARGELY UNMETHYLATED WITH AGING 52

7.3.1. Confirmation of extracted DNA quality 52

7.3.2. Confirmation of successful bisulfite conversion and Methylation-specific PCR 53

7.3.3. Confirmation of successful DNA cloning 54

7.3.4. Sequencing and analysis reveals that the rat SOD2 promoter region remains largely unmethylated with aging 56

8. DISCUSSION 59

8.1. MNSOD ACTIVITY AND REGULATION CHANGES WITH AGING 59

8.2. EPIGENETIC REGULATION OF MNSOD IN THE AGING CONTEXT 67

8.3. CONCLUSION 74

9. REFERENCES 75

10. APPENDICES 84

10.1. Appendix A 84

10.2. Appendix B 85

10.3. Appendix C 89

1. LIST OF FIGURES, TABLES AND ABBREVIATIONS

1.1. LIST OF FIGURES

Figure 1. Rat SOD2 promoter annotation illustrating species conservation and GC frequency……41

Figure 2. Comprehensive putative annotation of the rat SOD2 gene promoter region……42

Figure 3. Gel electrophoresis images of extracted total RNA……44

Figure 4. Melting curve of SOD2, confirming target specificity……45

Figure 5. Melting curve of CCT4, confirming target specificity……46

Figure 6. Melting curve of RAB11B, confirming target specificity……46

Figure 7. Melting curve of RPN1, confirming target specificity……47

Figure 8. Standard curve for SOD2……48

Figure 9. Standard curve for CCT4……48

Figure 10. Standard curve for RAB11B……49

Figure 11. Standard curve for RPN1……49

Figure 12. RT-PCR reveals increased SOD2 mRNA levels in tissues from old rat liver compared to young rat liver……51

Figure 13. RT-PCR reveals decreased SOD2 mRNA levels in tissues from old rat brain compared to young rat brain……52

Figure 14. Gel electrophoresis image of extracted whole genomic DNA……55

Figure 15. Successful MS-PCR amplification using primers for rat SOD2 promoter regions 1A and 1D……56

Figure 16. Enzyme digestions of recombinant plasmid samples indicate successful DNA cloning……57

Figure 17. Multiple sequence alignment of rat SOD2 promoter region 1A and the unconverted DNA sequence illustrates that the rat SOD2 promoter remains largely unmethylated in aging brain tissue……59

Figure 18. Multiple sequence alignment of rat SOD2 promoter region 1D and the unconverted DNA sequence illustrates that the rat SOD2 promoter remains largely unmethylated in aging brain tissue……60

1.2. LIST OF TABLES

Table 1. Primer sequences used in RT-PCR……29

Table 2. PCR cycling conditions for melting curve analysis……32

Table 3. Standard RT-PCR cycling conditions……34

Table 4. Primer sequences used in MS-PCR……36

Table 5. MS-PCR cycling conditions……38

Table 6. Efficiency of gene amplification……50

Table 7. t-Test for liver RT-PCR data confirms that differences in mRNA levels are statistically insignificant……53

Table 8. t-Test for brain RT-PCR data confirms that differences in mRNA levels are statistically insignificant……53

1.3. LIST OF ABBREVIATIONS

ROS - reactive oxygen species

ETC - electron transfer chain

$\cdot O_2^-$ - superoxide anion

H_2O_2 - hydrogen peroxide

$^1O_2$ - singlet oxygen

·OH - hydroxyl radical

G - guanine

T - thymine

AD - Alzheimer's disease

Aβ - amyloid-beta

SOD - superoxide dismutase

GSH-Px - glutathione peroxidase

CAT - catalase

Cu/ZnSOD - cytosolic copper-zinc superoxide dismutase

MnSOD - mitochondrial manganese superoxide dismutase

ECSOD - extracellular superoxide dismutase

SOD2 - MnSOD-encoding gene

hAPP - human amyloid precursor protein

SOD1 - Cu/ZnSOD-encoding gene

CpG - cytosine, guanine dinucleotide

CGI - CpG island

5’ - five prime

MBD - methyl-binding domain protein

APP - beta-amyloid precursor protein

GC - guanine and cytosine dinucleotide

Sp1 - specificity protein one

AP-2 - activating protein two

HSS - hypersensitive site

bp - base pairs

mRNA - messenger RNA

UCSC - University of California, Santa Cruz

RT-PCR - reverse transcription quantitative polymerase chain reaction

NCBI - The National Centre for Biotechnology Information

3’ - three prime

cDNA - complementary DNA

CP - crossing point

E - efficiency

NRTC - no reverse transcription control

NTC - no template control

SD - standard deviation

SE - standard error

n - sample size

MS-PCR - methylation-specific polymerase chain reaction

dNTP - deoxynucleotide

IPTG - Isopropyl β-D-1-thiogalactopyranoside

X-gal - 5-bromo-4-chloro-3-indolyl-beta-D-galacto-pyranoside

TSS - transcription start site

UTR - untranslated region

HDACs - histone deactylases

HMTs - histone methyltransferases

TFBS - transcription factor binding sites

TAE – Tris base, acetic acid & EDTA

2. ABSTRACT

The free radical theory of aging postulates that accumulation of oxidative damage in major cellular components is the predominant underlying cause of the aging phenotype. This damage is caused most commonly by reactive oxygen species (ROS) and antioxidant enzymes such as the superoxide dismutases (SOD) that neutralize ROS, are therefore vital. Manganese superoxide dismutase (MnSOD) is particularly critical as it is functional in the mitochondria, a major site for ROS generation. Numerous studies have demonstrated a tissue-specific decrease in the activity and mRNA levels of major antioxidants, including MnSOD, with aging, however the exact mechanism of this regulation is unclear. It was hypothesized that a general down-regulation of various antioxidant enzymes such as this may occur at the transcriptional level. In order to investigate SOD2 regulation, a comprehensively annotated rat SOD2 promoter region was established using the appropriate bioinformatics tools. Following this, SOD2 mRNA levels in tissues from young and old rat tissue were compared using quantitative PCR. The results showed increased and decreased SOD2 mRNA levels in old compared to young liver tissue and brain tissue, respectively, however these trends were not statistically significant. As MnSOD has been shown to be epigenetically downregulated in various age-related diseases it was hypothesized that the decrease in MnSOD mRNA levels seen in aging brain tissue may be a result of epigenetic regulation at the SOD2 (MnSOD gene) promoter, specifically, through DNA methylation. A methylation assay assessing the SOD2 gene promoter revealed no significant evidence of hypermethylation. Although this suggests that promoter methylation is an unlikely mechanism of SOD2 regulation in aging, further work would need to be implemented in order to prove this conclusively.

3. INTRODUCTION

3.1. AGING, AGE-RELATED DISEASE AND THE FREE RADICAL THEORY

Aging is generally defined as a gradual deterioration of an individual's overall physiological capacity as well as cellular function, such that they are more susceptible to developing a variety of illnesses and have reduced probability of survival (D'Aquila et al., 2012). There are a number of diseases that show an age-related prevalence, including certain cancers, cardiovascular disease, and neurodegenerative conditions such as Alzheimer's and Parkinson's disease (Valko et al., 2007; Gupta et al., 2014). At the molecular level, aging can be described as the progressive accumulation of damage to major cellular components such as nucleic acids, proteins and lipids, leading to increased cellular senescence and cell death (Rattan, 2006; Rai & Troen, 2011). There is no universally accepted biological theory of aging to date, however a number of partially explanatory theories have been put forward. Of these, the free radical theory of aging is possibly the most widely accepted and well established.

The free radical theory of aging was first proposed in 1956 by Denham Harman and has since gained large traction in the biogerontological community. This theory claims that the aging phenotype is related to the accumulation of oxidative damage to various cellular components as a result of aerobic metabolism (Wickens, 2001; Liochev, 2013). The damaging species implicated in this process are collectively referred to as reactive oxygen species (ROS) and are generated predominantly as by-products of the mitochondrial respiratory chain, but can result from environmental sources such as ultra violet light, ionizing radiation and some pollutants (Wickens, 2001). In the electron transfer chain (ETC), oxygen is reduced to water in four sequential steps. It is, however, possible for electrons in this chain to be leaked, and react with other intermediates, leading to the formation of free radicals and subsequently ROS (Raha & Robinson, 2000; Barja, 2013). Mitochondria are extremely vulnerable to damage mediated by ROS as they constitute the predominant site of oxygen metabolism (Kirkinezos & Moraes, 2001; Barja, 2013). Mitochondrial DNA lacks protective histone proteins and is in close proximity to the ETC situated

on the inner mitochondrial membrane, making it a major target for oxidative damage. This damage is not repaired as efficiently as in nuclear DNA, thus leading to elevated levels of mutagenesis (Alexeyev, Doux, & Wilson, 2004; Barja, 2013). In general, oxidative damage to mitochondrial DNA as well as lipid peroxidation in the mitochondrial membranes lead to a reduction in ATP production and further generation of ROS and cytotoxicity, events that are suggested to be fundamental to the aging phenotype (Alexeyev, Doux & Wilson, 2004; Barja, 2013).

The major free radical implicated in ROS production is the superoxide anion ($\cdot O_2$-), formed when an oxygen molecule accepts an additional electron (Flint, 1993). Superoxide itself can have toxic effects, however its more harmful role is in the generation of other ROS. Superoxide reacts with hydrogen to form hydrogen peroxide (H_2O_2) and singlet oxygen ($^1O_2$, a non-radical, excited form of oxygen) in two separate reactions (Lee, Koo, & Min, 2004). These ROS have been implicated in various forms of macromolecular damage and contribute to the production of more toxic ROS such as the hydroxyl radical (·OH) (Lee, Koo & Min, 2004). The hydroxyl radical is highly reactive and can cause direct oxidative damage to proteins, lipids and DNA. In DNA, ·OH can react with DNA bases and the deoxyribose backbone leading to mutations and genomic instability (Valko et al., 2007; Gupta et al., 2014). In proteins, oxidation of amino acid side chains (particularly of methionine and cysteine) can lead to the production of disulphide bonds between thiol groups and can also lead to other detrimental effects. Finally, lipid peroxidation can lead to irreversible impairment of the phospholipid membrane fluidity and elasticity which can result in rupturing of the cell membrane (Wickens, 2001; Matés et al., 2012). Other toxic ROS include peroxyl and alkoxyl radicals and peroxynitrate, reactive substances that also play a significant role in oxidative damage to cellular macromolecules (Lee, Koo & Min, 2004).

A large body of evidence has demonstrated that cellular levels of these oxidative lesions increase with age (Harman, 2006; Lee et al., 2004; Matés, 2000; Raha & Robinson, 2000; Barja, 2013; Liochev, 2013). This and other lines of evidence, including studies on correlations of species life span, metabolic rate and antioxidant activity as well as life span extension by calorie restriction

(which leads to a decline in the production of ROS), contribute convincing evidence in support of the free radical theory of aging (Wickens, 2001; Lin et al., 2002; Balaban, Nemoto & Finkel, 2005; Hulbert et al., 2007; Barja, 2013; Liochev, 2013).

In addition to the general condition of aging, ROS have been implicated in a number of age-related diseases, including various sporadic cancers and neurodegenerative conditions (Valko et al., 2007; Gupta et al., 2014). Accumulative damage to DNA is now known to be a major cause of cancer (Waris & Ahsan, 2006; Matés et al., 2012). As ROS can directly damage DNA it is considered both a mutagenic and carcinogenic factor (Loft & Poulsen, 1996). Additionally, ROS accumulates with age in a manner that may predispose an individual to late-onset tumourigenesis. An important oxidative DNA lesion is 7,8-dihydro-8-oxoguanine, which leads to G to T transversion mutations. This kind of mutation is frequent in various cancers and is the most common mutation in the p53 tumour suppressor gene (Hollstein, et al., 1991). This and other damage caused by oxidative modifications to DNA (including single and double strand breaks and DNA cross-links) can occur in proto-oncogenes and tumour suppressor genes, leading to neoplastic formation (Valko et al., 2007). Additionally, ROS have been implicated in signaling pathways central to tumourigenesis and various lines of antioxidant defenses, including free radical scavengers, have been shown to have aberrant expression patterns in a number of cancers (Valko et al., 2007; Gupta et al., 2014).

Based on *in vitro* and *in vivo* studies of Alzheimer's disease (AD), amyotrophic lateral sclerosis (ALS), as well as other neurodegenerative conditions, aging and mitochondrially-generated ROS accumulation may play a large role in the initiation and progression of these late-onset diseases (Reddy, 2009; Sutherland et al., 2013). The brain is particularly vulnerable to oxidative damage due to its high oxygen usage, high content of polyunsaturated fatty acids and availability of redox metals (Valko et al., 2007). As a consequence of this, neurons are highly sensitive to oxidative damage which subsequently leads to neuronal cell death, a unifying mechanism in neurodegeneration (Ischiropoulos & Beckman, 2003). The brains of AD patients show a significant accumulation of amyloid-β (Aβ) peptide, a major component of aberrant plaques that

deposit in vital regions of the brain (Butterfield, et al., 2002; Sutherland et al., 2013). It is postulated that Aβ may serve as an antioxidant for brain lipoproteins and increased production of Aβ as a result of oxidative stress in aging is a critical event in AD progression (Butterfield, et al., 2002; Sutherland et al., 2013). This and other research provides strong evidence for the association of aging, oxidative damage and neurodegeneration.

3.2. ANTIOXIDANT DEFENSES IN AGING, CANCER AND NEURODEGENERATIVE DISEASE

In order to minimize accumulation of ROS, and the detrimental effects it is associated with, aerobic organisms have developed complex defense mechanisms, the forefront of which are the antioxidant enzymes superoxide dismutase (SOD), glutathione peroxidase (GSH-Px) and catalase (CAT) (Lee, Koo & Min, 2004). CAT is a highly efficient enzyme that converts hydrogen peroxide into water and molecular oxygen (Matés, 2000). Together with GSH-Px, which catalyzes the reduction of a variety of hydroperoxides using glutathione, CAT neutralizes potentially toxic cellular hydrogen peroxide generated by the SOD enzymes (Matés, 2000). Superoxide dismutases are specialized in neutralizing superoxide anion radicals by converting them into hydrogen peroxide and molecular oxygen (Miao & Clair, 2009). Three SOD enzymes have been characterized in mammals thus far: cytosolic copper-zinc superoxide dismutase (Cu/ZnSOD), mitochondrial manganese superoxide dismutase (MnSOD) and extracellular superoxide dismutase (ECSOD). Of these, MnSOD appears to be the most vital, as demonstrated by early lethality of homozygous SOD2 knockout mice, compared to the non-lethal effects of Cu/ZnSOD and ECSOD knockouts (Huang et al., 1997). Additionally, mice showing MnSOD deficiency are more susceptible to several forms of oxidative stress and cellular senescence (Velarde et al., 2012) and overexpression of MnSOD in cultured cells renders cells resistant to oxidant-induced cytotoxicity and radiation-induced neoplasm (Matés, 2000). As the mitochondria are the predominant source of superoxide, and are the organelles most sensitive to its effects, it follows that mitochondrial MnSOD is the most critical of the SOD enzymes.

The protective effects of the antioxidant enzymes as well as other antioxidant defenses are formidable, and minimal steady state levels of ROS are maintained in healthy individuals (Matés, 2000; Matés et al., 2012). It is when the generation of oxidants exceeds this dynamic defense system, that cellular and physiological decline ensues. Naturally, the oxidant/antioxidant balance may be perturbed by one of two events: an overall increase in ROS production or a systematic decrease in the activity of the cell's antioxidant armory. With this in mind, as well as the significant increase of oxidative damage with aging, and the major role ROS play in various age-related diseases, it follows that the activity of important antioxidant enzymes has been investigated in the context of aging, as well as in disease progression.

The age-related activity of antioxidant enzymes has been assayed in a number of tissues of both human and rodents with varying results. Cand and Verdetti (1989) demonstrated that SOD activities decrease significantly for the aged liver and kidney in rats. This finding was supported by Rao, Xia and Richardson (1990) who found an age-related decrease in SOD activity in rat brain, heart, hepatocytes, intestinal mucosa and kidney. A further study by Navarro and Boveris (2004) showed a progressive decrease in MnSOD activity in the mitochondria of rat brain and liver. Contrary to this Yen et al. (1994) demonstrated an increase in SOD activity in the mitochondria of human liver. It is possible that discrepancies in these findings may be due to different technical approaches, however a large portion of research to this end suggests that SOD activity does in fact decrease in a tissue-specific manner as a function of age, consistent with the age-related increase in cellular levels of the superoxide anion radical and the damage it inflicts.

In neurodegenerative studies, superoxide dismutase, catalase and glutathione peroxidase have been demonstrated to have reduced activity in brains of AD patients (Marcus et al., 1998). Additionally, in mice transgenically expressing hAPP (human amyloid precursor protein), SOD2 is found highly expressed around amyloid plaques but is decreased in AD brains overall (Esposito et al., 2006). Abnormal SOD2 expression has also been associated with Huntington's disease, where surviving neurons have strongly induced expression of the antioxidant (Ischiropoulos & Beckman, 2003). This finding was validated in a study that showed that MnSOD can prevent

neural apoptosis and reduce ischemic brain injury (Keller et al., 1998). Downregulation of SOD1, the gene encoding for Cu/ZnSOD, in mice and in cells is also associated with increased neurodegeneration and neural death. Mutations in the SOD1 gene have been frequently detected in ALS and may represent an initiating factor in this disease (Ischiropoulos & Beckman, 2003). Finally, in cancer, MnSOD has been described as a putative tumour suppressor gene due to its demonstrated downregulation in various cancer types (Hitchler et al., 2006; Hodge et al., 2005; Huang, He & Domann, 1999). These findings suggest that the balance between ROS and cellular antioxidant defenses such as the SOD proteins may be crucial in the progression of aging, cancer and neurodegeneration.

It appears that decreased activity of major antioxidants may play a significant role in the accumulation of oxidative damage in aging and age-related disease. A decrease in enzyme activity can be caused by a number of factors at the transcriptional, translational and post-translational levels. However, it is probable that this kind of age-related, large-scale down-regulation of key antioxidant genes is mediated at the transcriptional level, in a systematic manner. Regulation of this description frequently falls under the category of epigenetics.

3.3. EPIGENETIC TRENDS IN AGING, CANCER AND NEURODEGENERATIVE DISEASE

“Epigenetics” refers to a form of transcriptional regulation of the genome mediated by modifications to the chromatin structure of DNA and histone proteins. These modifications can be stable or transient and are heritable through mitosis and sometimes, meiosis (Holliday, 2006). The compact organization of chromatin determines the accessibility of gene regions to the transcriptional machinery, thereby regulating their activation or repression. Common epigenetic mechanisms include DNA methylation, alterations of histone proteins and small non-coding RNAs (Holliday, 2006).

DNA methylation involves the covalent attachment of a methyl group to the carbon 5 of a cytosine residue positioned in a CpG dinucleotide. CpG dinucleotides are found unevenly

distributed across the human genome, however they can be found in regions of high concentration, referred to as 'CpG islands' (CGIs) (Illingworth & Bird, 2009). CGIs can be found in approximately 50% of human genes, located upstream of the gene promoter (Illingworth & Bird, 2009). Most of the CpG sites dispersed sporadically throughout the genome are highly methylated, however, CGIs within gene promoter regions remain largely unmethylated (Klose & Bird, 2006). Upon the rare occurrence of promoter CGI methylation, the induction of long term transcriptional silencing ensues. DNA methylation can lead to gene repression directly, by preventing the binding of transcription factors through steric hindrance, or indirectly, by recruiting various methyl-binding domain proteins (MBDs) (Holliday, 2006). MBDs can interact with enzymes such as histone deactylases and histone methyltransferases to synergistically reconfigure the chromatin structure and promote repression of gene expression (Holliday, 2006).

Global epigenetic patterns are established at the pre-conceptional period and are later reprogrammed during embryogenesis and cell differentiation. However, these patterns can undergo alterations throughout an organism's lifetime, in response to exogenous and endogenous stimuli (Aquila et al., 2012). In fact, a large body of research has established numerous epigenetic patterns that appear to change with age, indicating that epigenetic modifications may contribute to or be a result of this phenotype (Aquila et al., 2012; Vlaming & Leeuwen; Gentilini & Castaldi, 2012). In general, a progressive loss of total methylated cytosine with age has been demonstrated in most vertebrate tissues (Richardson, 2003). This hypomethylation is localized mainly in non-island CpGs dispersed over repetitive gene sequences (Jintaridth & Mutirangura, 2010). In contrast, during aging, a robust rise in levels of DNA methylation at specific gene promoters has been described (Gentilini, et al., 2012; Winnefeld & Lyko, 2012). This promoter hypermethylation has been detected in genes for tumour suppression (p16INK4A, RASSF1), metabolism (ECRG4, ATP13A4) and DNA repair (MLH1, BRCA1) amongst others (Gentilini, et al., 2012; Winnefeld & Lyko, 2012). These findings suggest that there is a loss of epigenetic control that accompanies aging. This epigenetic drift may predispose an individual to age-related diseases and other detrimental symptoms of aging through the reactivation of

potentially mutagenic sequences (e.g., transposons and repetitive sequences) and the inactivation of important housekeeping genes (Aquila et al., 2012).

This theory is supported by similar epigenetic changes seen in the epigenomes of cancer patients. As in aging, there are two predominant aberrant methylation patterns observed – global DNA hypomethylation and promoter-specific hypermethylation (Herman & Baylin, 2003; Ehrlich, 2002; Soo You & Jones, 2012). In cancer, gene silencing through DNA methylation is a common mechanism for the repression of tumour-suppressor genes as well as DNA repair enzymes (Jones and Baylin, 2007; Toyota & Issa, 1999; Soo You & Jones, 2012). Conversely, a loss in DNA methylation can have equally detrimental effects. Similar to the aged epigenome, global hypomethylation may lead to genomic rearrangements caused by expression of repeat sequences and reactivation of previously silenced genes and DNA elements (Tsai & Baylin, 2011).

Aberrant epigenetic patterns have also been detected in a number of neurological diseases, including Alzheimer's. The sporadic origin of up to 90% of AD cases, the vast differences in individual susceptibility and disease manifestations as well as the age-related onset of the disease suggest that environmental and epigenetic mechanisms may play a major role in sporadic AD etiology (Zawia, Lahiri & Cardozo-Pelaez, 2009). It has been postulated that epigenetic mechanisms promoting the accumulation of oxidative damage in the brain may be a major initiating factor in AD. DNA methylation patterns analyzed in prefrontal cortex and lymphocytes from late-onset AD patients, revealed age-specific epigenetic drift characterized by unusual methylation patterns (Wang, Oelze, & Schumacher, 2008). Specifically, promoter hypomethylation of genes associated with AD, such as the beta-amyloid precursor protein (APP) may lead to the increased levels of APP and Aβ and subsequent ROS production seen in AD brains. Conversely, other AD-associated genes appear to be repressed late in life, suggesting that promoter hypermethylation may contribute to AD (Zawia et al., 2009).

The similarities in patterns of epigenetic change seen in aging and cancer and the age-related epigenetic drift seen in AD may provide insight into the mechanism through which aging confers an increased risk for age-related disease progression. Analysis of the promoter methylation of a

number of tumour-suppressor and tumour-related genes from non-cancerous autopsy samples has revealed that methylation occurs in these genes in an age-related and tissue specific manner, suggesting that age-related methylation may constitute a mutator process (Waki, Tamura, Sato, & Motoyama, 2003). As mentioned, the accumulation of ROS is a phenomenon seen in aging and age-related disease and may be a result of the progressive down-regulation of various antioxidant enzymes. In theory, it is possible that this down-regulation is due to aberrant epigenetic patterns, specifically, repressive epigenetic modifications at gene promoters. This would result in an age-related accumulation of ROS, which in turn, renders an individual particularly vulnerable to age-related disease. Indeed, aberrant epigenetic regulation of MnSOD, the most vital of the superoxide dismutases and antioxidant enzymes, has been demonstrated in various age-related diseases.

3.4. EPIGENETIC REGULATION OF MNSOD IN DISEASE

The complete genomic structure for SOD2 has been determined for the human (Wan et al., 1994), rat (Ho, Howard & Crapo, 1991) and mouse (Jones et al., 1995) with all of these species showing marked conservation of structure and sequence. The SOD2 gene promoter does not contain TATA or CAAT boxes but does include GC-rich motifs, promoter properties that are characteristic of housekeeping genes. The GC-rich motifs are contained within a large CpG island (approximately 3.5 kb in length) that spans the promoter and extends into intron two (Wan et al., 1994; Ho, Howard & Crapo, 1991; Jones et al., 1995). This region appears to be highly conserved across mouse, rat and human (Wan et al., 1994; Ho, Howard & Crapo, 1991; Jones et al., 1995). A promoter fragment 500 bp upstream of the transcription start site of the human SOD2 gene has been identified as the most critical for basal transcription levels of SOD2 and contains multiple putative binding-sites for transcription factors Sp1 (specificity factor 1) and AP-2 (activating protein 2) (Xu, Porntadavity & St Clair, 2002).

In addition to the 5' basal promoter region, an inducible enhancer region has been localized to a 260 bp fragment in intron two in both the rat and human genes (Rogers et al., 2000). The intronic enhancer contains binding sites for NF-κB, C/EBP and NF-1 and possesses the ability to promote

cytokine-inducible transcription independent of a promoter sequence (Rogers et al., 2000). It is through this enhancer that Mn-SOD expression is dramatically regulated by numerous proinflammatory mediators, including tumor necrosis factor-A and interleukin-1 (Kuo et al., 1999).

Interestingly, the consensus binding sequences for both Sp1 and AP-2 are GC-rich and methylation of one or more of these sites has been shown to be responsible for the reduced levels of SOD2 in cancer (Hodge et al., 2005; Hitchler et al., 2006). Additionally, the NF-κB and NF-1 binding sites located within the SOD2 intronic enhancer both contain a GC-dinucleotide and aberrant methylation associated with reduced SOD2 levels has also been found in this region in pulmonary arterial hypertension and cancer (Archer et al., 2010; Huang, He & Domann, 1999). Additionally, Thaler et al. (2009) showed that diet has an impact on promoter methylation of MnSOD.

The discovery that SOD2 may undergo epigenetic regulation in the progression of lifestyle diseases such as cancer and hypertension and in response to diet, suggests that epigenetic modification may underlie the age-related decrease in activity of MnSOD demonstrated in a number of studies (Cand & Verdetti, 1989; Rao, Xia and Richardson, 1990; Navarro and Boveris, 2004). As mentioned, hypermethylation of various genes for tumour suppression, metabolism and DNA repair have been demonstrated in aging (D'Aquila et al., 2012), suggesting that epigenetic downregulation of key housekeeping genes may be a general trend in the aging phenotype and may contribute to the an individual's susceptibility to age-related diseases such as cancer and neurodegeneration. To date, the epigenetic regulation of MnSOD has not been explored in the context of aging.

This leads to the hypothesis that the decreased activity of SOD2 seen in aging and age-related disease is due to epigenetic downregulation of the SOD2 gene through promoter CpG hypermethylation.

4. SIGNIFICANCE OF THIS WORK

This research will address a novel aspect of the free radical theory of aging, epigenetic down-regulation of antioxidant genes, as well as improve our understanding of an individual's susceptibility to aging and age-related disease. Additionally, novel markers of this susceptibility may be elucidated, which could create opportunity for early detection of disease risk (e.g. in breast cancer and Alzhiemer's disease) as well as for therapy aimed at altering the reversible state of aberrant epigenetic modifications.

5. HYPOTHESIS, AIM AND OBJECTIVES

5.1. HYPOTHESIS

It is hypothesized that the expression of SOD2 is downregulated as a function of age in rat brain and liver tissue and this downregulation is facilitated by the epigenetic mechanism of promoter hypermethylation.

5.2. AIM AND OBJECTIVES

This project aims to investigate the epigenetic regulation of the SOD2 gene with age.

Objective 1. Investigate the putative transcriptional and epigenetic regulatory sites in the rat SOD2 gene promoter using appropriate bioinformatics tools.
Objective 2. Quantify and compare levels of SOD2 mRNA in extracts from young and old rat brain and liver tissue.
Objective 3. Quantify and compare promoter methylation of the SOD2 gene in extracts from young and old rat brain tissue.

6. MATERIALS AND METHODS

6.1. SOD2 PROMOTER ANNOTATION

6.1.1. Basic SOD2 gene annotation

The rat manganese superoxide dismutase gene promoter from the RGSC 5.0/rn5 Assembly, chr1:51,827,380-51,834,232, was investigated using the UCSC genome browser (https://genome.ucsc.edu/) and the WashU EpiGenome Browser (http://epigenomegateway.wustl.edu/browser/). Both sites generate results illustrating the genes position relative to the chromosome, exonic and intronic structure, GC frequency and the presence of CGIs and these results were compared for consistency.

6.1.2. PATCH analysis

In order to explore possible regulatory sites located within the rat SOD2 gene promoter a predictive transcriptional regulatory site analysis was performed using PATCH, a Gene-Regulation tool, (http://www.gene-regulation.com/pub/programs.html#patch). PATCH is a pattern-based program for predicting transcription factor binding sites (TFBS) in DNA sequences. PATCH makes use of TRANSFAC (developed by the former German National Research Centre for Biotechnology), a database that contains information on eukaryotic transcription factors, their genomic binding sites and DNA binding profiles. The gene sequence used in this analysis was obtained from the UCSC genome browser, RGSC 5.0/rn5 Assembly, chr1:51,827,380-51,834,232.

6.1.3. Comprehensive SOD2 promoter annotation

In addition to these analyses, which were mapped to the rat SOD2 promoter sequence using LaserGene SeqBuilder (www.dnastar.com), a manual comparison of the rat and annotated human and mouse SOD2 sequences was performed using the consensus sequences for binding of Sp1, AP-2 and other transcription factors as well as experimental data reporting putative protein

binding sites based on DNAse I-Hypersensitive site analysis (Kuo et al., 1999). These results were coupled with those generated by the UCSC genome browser, WashU EpiGenome Browser and the PATCH analysis to delineate the putative transcriptional and epigenetic regulatory sites in the rat SOD2 gene promoter. This putative annotation of the rat SOD2 promoter region allowed for the elucidation of promoter elements that may be affected by abnormal methylation and that could be targeted in a methylation assay.

6.2. REVERSE TRANSCRIPTION QUANTITATIVE PCR (RT-PCR)

Quantitative PCR allows researchers to monitor the amplification of nucleic acid indirectly through the quantification of fluorescence (Roche Lightcycler® Real-Time PCR Systems Application Manual). SYBR Green I, a molecule that becomes incorporated by double-stranded DNA and subsequently fluorescence is a commonly used in this technique (Roche Lightcycler® Real-Time PCR Systems Application Manual). The incorporation and fluorescence of SYBR Green I in solution increases proportionally as the amount of double-stranded DNA increases through consecutive rounds of PCR amplification. By plotting this accumulative fluorescence data against the number of PCR cycles (an amplification curve), it is possible to elucidate the cycle at which fluorescence of target DNA rises above baseline fluorescence, or the crossing point (CP). The CP of a target molecule is dependent on the initial concentration of DNA that was present in solution (this relationship is inversely proportional), and can therefore be used to quantify the amount of nucleic acid in a sample (Roche Lightcycler® Real-Time PCR Systems Application Manual). In order to quantify subtle changes in nucleic acid between samples, it is recommended that relative quantification is performed, where the initial concentration of nucleic acid in a sample is not quantified absolutely, but in relation to the initial concentration of other reference nucleic acid targets (Roche Lightcycler® Real-Time PCR Systems Application Manual).

6.2.1. Primer design

All primer sets synthesized for use in RT-PCR were designed with PrimerBlast (www.ncbi.nlm.nih.gov/tools/primer-blast/) and met the following specifications; amplicons

were 80 – 200 bp and spanned an exon/intron boundary, primers were between 18 and 22 bp in length, GC content fell within the range of 50 – 60 %, annealing temperatures fell within the range of 55 – 65 ˚C and self-complementarity and secondary structure of primers was not significant. Primers were also assessed for specificity using a NCBI BLAST analysis (http://blast.ncbi.nlm.nih.gov/Blast.cgi). The primer set targeting rat SOD2 mRNA was based on the NCBI sequence NM_017051.2. Additionally, primers were designed for rat RAB11B (NM_032617.2), RPN1 (NM_013067.1) and CCT4 (NM_182814.2), three reference genes selected using RefGenes from from Genevestigator (http://refgenes.org/). Refgenes is an online application that allows users to search for reference genes that are constitutively expressed across a chosen set of samples (including organism, tissue and genetic and physiological characteristics) based on microarray data. Additionally, reference genes chosen show similar expression profiles to the target gene across samples, an important consideration in RT-PCR. The validity of these assumptions was assessed by the reproducibility of the RT-PCR data gathered for all reference genes as well as by the precision of the inter-assay results.

Primers were synthesized by Inqaba Biotech and were isolated using Reverse-phase cartridge purification. Forward and reverse primer sequences for SOD2, RAB11B, RPN1 and CCT4 are shown below.

Table 1. Primer sequences used in RT-PCR.

Gene Name	Primer sequences	Amplicon size (bp)
SOD2	Forward: 5’- CCCAAAGGAGAGTTGCTGGAG -3’ Reverse: 5’- CTGTAAGCGACCTTGCTCCT -3’	144
CCT4	Forward: 5’- ATGTCCGAAAGGGTGGGATCT -3’ Reverse: 5’- CTCCGCACAGTTTCAGTTGC -3’	103
RAB11B	Forward: 5’- ATTCAGGTGGACGGCAAGAC -3’ Reverse: 5’- CGGTAGTACGCAGAGGTAATGG -3’	89
RPN1	Forward: 5’- GAAGGGGAAAAGTGGGAGGT -3’ Reverse: 5’- GTCGGGTATGGATGAAGCACA -3’	117

6.2.2. RNA extraction

3 young (1 to 2 months) and 3 old (15 to 19 months) healthy Sprague-Dawley rats were provided by WITS Central Animal Service and were euthanized with pentobarbitone. This was in accordance with the ethical clearance certificate 2014/33/O issued by the Animal Ethics Screening Committee (June 2014). Pentobarbitone overdose was chosen instead of the more common CO_2-induced euthanasia as the specific oxygen environment of the cell has biological influences on SOD2 expression (Dioum et al., 2009). Pentobarbitone is a barbiturate that interferes with neurotransmitter receptor signalling in the central nervous system, and does not significantly affect SOD2 expression (Bette et al., 2004). The old rats were designated rat A, C and D and the young rats were designated rat B, E and F. Snap frozen tissue was stored at – 80 ˚C for a period of up to 12 months. Prior to RNA extraction tissues were homogenized using Zymo Research's BashingBead™ Lysis Tubes in a guanidine thiocyanate and β-mercaptoethanol-containing RNA Lysis Buffer (provided with below mentioned kits). Total RNA was extracted from fresh or snap frozen young and old rat brain and liver tissue using Promega's SV Total RNA Isolation System and/or Macherey-Nagel's NucleoSpin® RNA isolation kit, according to manufacturer's instructions. The amount of tissue processed in each reaction was standardized to 30 mg for liver tissue and 60 mg for brain tissue and an average of two RNA samples were extracted from each rat for each tissue (liver and brain). Prior to RNA elution each spin column was incubated with a solution of DNAse I (Cat.# Z3105) and 0.09M $MnCl_2$ to degrade contaminating genomic DNA. RNA was eluted and stored in nuclease-free water at – 80 ˚C. RNA eluents were quantified and assessed for purity using a NanoDrop-1000 spectrophotometer by ensuring that the 280/260 and 230/260 ratios fell within the acceptable range of 1.8 to 2.2. Furthermore, before use in cDNA synthesis, all RNA eluents were assessed using agarose gel electrophoresis and the Bio-Rad Gel Doc XR System with Image Lab™ Software to confirm the absence of significant degradation. RNA was resolved with the Fermentas GeneRuler 1kB (molecular weight range 250 bp to 10000 bp) for 20 minutes at 100 V on a 10 % agarose gel (prepared with GRGreen nucleic acid stain) in a TAE buffer system.

6.2.3. Reverse transcription

RNA was converted into cDNA using the RevertAid First Strand cDNA Synthesis kit (Thermo Scientific), according to manufacturer's instructions. Input RNA was standardized to a concentration of 100 ng/µl of total reaction mix (20 µl) and an Oligo$(dT)_{18}$ priming strategy was used. This kit makes use of the RevertAid M-MuLV Reverse Transcriptase which has relatively low RNAse H acitivity and the RiboLock™ RNAse Inhibitor which effectively protects RNA from degradation. The reaction mix was incubated at 42 ˚C for 60 minutes during cDNA synthesis and then at 70 ˚C for 5 minutes for reaction termination. cDNA synthesis was performed using two separate RNA samples from each rat, for brain tissue and one RNA sample from each rat, for liver tissue.

6.2.4. Quantitative PCR

cDNA used in all quantitative PCR reactions was synthesized no more than 4 hours prior to RT-PCR. The standard reaction used in all the RT-PCR performed was as follows; 2X Maxima SYBR Green qPCR Master Mix (Thermo Scientific), 0.3 µM reverse and forward primer, 100 ng cDNA and nuclease-free water made up to 25 µl. The master mix is comprised of Maxima Hot Start *Taq* DNA Polymerase, Maxima SYBR Green qPCR Buffer (with KCL, $(NH_4)_2SO_4$ and optimized $MgCl_2$ concentration), SYBR Green I and dUTP. Reactions were loaded into white Thermo-Fast® 96 well, low profile plates (Thermo Scientific) and the plates were sealed with optically clear adhesive seals (Thermo Scientific). All RT-PCR experiments were performed on the Roche LightCycler® 480 Instrument with software version 1.0.

Melting curve analysis

During melting curve analysis, the fluorescence of the sample is monitored while the temperature is steadily increased (up to 95 ˚C) and is then dropped to 60 ˚C and increased to 95 ˚C once again. During the initial temperature increase the double-stranded DNA becomes single-stranded and the fluorescence decreases as SYBR green I is released. As the temperature decreases, the fluorescence increases once again and eventually peaks at the primer set's ideal annealing temperature. The resulting curve is converted to a first derivative plot of fluorescence as a function of time. Specificity of each primer set is illustrated by a single peak on the melting curve. Additional informative characteristics of the melting curve are the height and width of the peak. A relatively short peak is representative of "late amplification" of the target and may indicate a low efficiency of amplification, while a relatively wide peak can mask the presence of more than one specific target and should be further investigated. In order to evaluate the specificity of each primer set, melting curve analyses were performed in replicate or triplicate under the following conditions;

Table 2. PCR cycling conditions for melting curve analysis.

Step	**Temperature (˚C)**	**Duration (s)**	**Number of cycles**
Initial denaturation	95	600	1
Denaturation	95	15	40
Annealing	60	30	40
Extension	72	30	40
Melt	95	5	1
	60	30	1
	95	5	1

The cDNA used in these experiments was synthesized from RNA originating from rat A. The resulting curves were converted to first derivative plots (-dF/dT plotted as a function of T) using a *T*m Calling analysis and the melting curves were assessed.

Standard curve analysis

Standard curves are establishing by determining the CP values of a series of template dilutions. These values are then plotted against the log concentration of the template, generating a linear curve. The gradient of this curve is indicative of the PCR efficiency, where the theoretical efficiency maximum of 2 indicates that the amount of product doubles with each cycle (Bustin et al., 2009). By using a broad range of template dilutions (at least 3 orders of magnitude) the sensitivity and limit of detection can also be assessed. Finally, by performing the PCR in replicate, the precision of the standard curve can be determined (Roche Lightcycler® Real-Time PCR Systems Application Manual).

The cDNA used in these experiments was synthesized from RNA originating from rat A. Five standard concentrations of cDNA were prepared through serial dilution, each differing by one order of magnitude and together covering a range of approximately 0.01 ng/µl to 100 ng/µl. RT-PCR at each concentration with each primer set was run in triplicate and a calibration curve was created by plotting the average CP (crossing point) versus the order of magnitude using Excel. The average efficiency of each target or reference gene amplification was calculated using the calibration curve gradient and the standard formula $E = 10^{-1/slope}$. Additionally the correlation coefficient was calculated to assess the linear relationship between CP values and the decreasing order of magnitude. The RT-PCR parameters for these reactions and all subsequent reactions were as follows;

Table 3. Standard RT-PCR cycling conditions.

Step	Temperature (˚C)	Duration (s)	Number of cycles
Initial denaturation	95	600	1
Denaturation	95	15	40
Annealing	60	30	40
Extension	72	30	40

Data normalization

In order to establish the unknown relative concentration of SOD2 cDNA in samples generated from RNA samples (originating from liver and brain tissue of three old and three young rats) RT-PCR reactions for SOD2 and three reference genes were run in triplicate. Additionally, for each primer set and sample used, a no reverse transcriptase control (NRTC) and a no template control (NTC) was included to assess for the presence of non-specific signalling resulting from genomic DNA amplification or background signalling. A “young” tissue sample was selected for calibration in each category. As mentioned, relative quantification compares the mRNA levels of the target sequence to the reference sequences in a single sample (Roche Lightcycler® Real-Time PCR Systems Application Manual). The final result is expressed as a ratio that is meaningful only when compared between samples. Another level of normalization is necessary between samples and is usually implemented by designating one of the samples a ‘calibrator sample’. All other samples are compared to the calibrator sample to account for sample variability.

Using the CP values generated by these experiments as well as the efficiency values obtained from the standard curves of SOD2 and the three reference genes, the relative normalized ratio

of SOD2 in each sample was calculated according to the following formula (Roche Lightcycler® Real-Time PCR Systems Application Manual);

$$\text{Normalized relative ratio} = E_t^{\,CP\,(\text{target})\,\text{calibrator} - CP\,(\text{target})\,\text{sample}} \,/\, E_r^{\,CP\,(\text{reference})\,\text{calibrator} - CP\,(\text{reference})\,\text{sample}}$$

Where E_t is the efficiency of SOD2 amplification, and E_r is the average efficiency of RAB11, RPN1 and CCT4 amplification.

A total of three relative ratios each were obtained for samples derived from old rat liver tissue and young rat liver tissue and six relative ratios each were obtained for samples derived from old rat brain tissue and young rat brain tissue. The relative ratios were averaged for each category and the standard deviation (SD) was calculated using Excel. Based on the standard deviation, the standard error (SE) for each category was calculated with the following formula;

$$SE = \frac{SD}{\sqrt{n}}$$

Where n is the sample size.

The average relative ratios for each group (young rat liver tissue, old rat liver tissue, young rat brain tissue and old rat brain tissue) was plotted in a histogram using Excel, with SE bars included.

Statistical analysis

To assess whether the difference between the relative SOD2 ratios in young and old rat tissue was statistically significant, t-tests assuming equal variance and a value of alpha = 0.05 were used. The t-tests were performed using the Excel data analysis tool.

6.3. BISULFITE DNA CONVERSION AND METHYLATION-SPECIFIC PCR

Due to the rapid development of the field of epigenetics in recent years, the establishment of reliable assays that are used to monitor changes in the epigenetic environment has become of utmost importance (DeAngelis & Farrington, 2008). Although many techniques are now available to analyze changes in DNA methylation patterns, bisulfite modification of DNA still forms the foundation upon which most of these techniques are based (DeAngelis & Farrington, 2008).

6.3.1. Primer design

All primer sets synthesized for use in methylation-specific PCR were designed with Zymo Research's Bisulfite Primer Seeker (www.zymoresearch.com/tools/bisulfite-primer-seeker) and met the following specifications; amplicons were 80 - 200 bp in length and contained 4 to 8 CpG dinucleotides, primers contained not more than one CpG dinucleotide and several non-CpG cytosine residues. Primers were designed to target the SOD2 promoter region -300 bp upstream to +120 bp downstream of the transcription start site within the gene CpG island, based on the NCBI Gene ID: 24787. Primer sets were synthesized by Inqaba Biotech and were isolated using Reverse-phase cartridge purification. The sequences for two different primer sets targeting two separate promoter regions (designated region 1A and region 1D) are listed below;

Table 4. Primer sequences used in MS-PCR.

Gene Name	Primer sequences	Amplicon size (bp)
Promoter region 1A	Forward: 5'- AGAAGAGGYGGGGTTTAGTTTGAGGGTG -3' Reverse: 5'- AACAAAACRACACACAAAAAAAACC -3'	180
Promoter region 1D	Forward: 5'- GGGTTAGYGTTTAGTTGTGTTTTTG -3' Reverse: 5'- ACCCCRAACCCTACCACTTACCTACAC -3'	159

Region 1A is located approximately -283 to -103 bp relative to the SOD2 transcription start site and region 1D is located approximately -47 bp to 112 + bp relative to the transcription start site.

6.3.2. Genomic DNA extraction

Whole genomic DNA was extracted from snap frozen brain tissue (previously described) using the NucleoSpin® Tissue from Macherey-Nagel, according to manufacturer's instructions. The amount of tissue processed in each reaction was standardized to 60 mg. DNA quality was assessed using gel electrophoresis and the Bio-Rad Gel Doc XR System with Image Lab™ Software. DNA was resolved with the Fermentas GeneRuler 1kB (molecular weight range 250 bp to 10000 bp) for 45 minutes at 100 V on a 10 % agarose gel (prepared with GRGreen nucleic acid stain) in a TAE buffer system. Additionally, DNA quantity and purity was evaluated using a NanoDrop-1000 spectrophotometer by ensuring that the 280/260 and 230/260 ratios fell within the acceptable range of 1.8 to 2.2.

6.3.3. Bisulfite conversion

This experiment made use of the EZ DNA Methylation-Startup™ Kit (Zymo research). This required approximately 200 ng of extracted DNA to be made up to a volume of 20 µl with nuclease-free water. This solution was then incubated at 98 ˚C for 8 minutes and at 64 ˚C for 3.5 hours with the bisulfite-containing Conversion Reagent. Bisulfite induces the conversion of all unmethylated cytosines into uracil, while methylated cytosines remain unchanged. After incubation, DNA was isolated through a NucleoSpin® Tissue Column, washed, desulphonated and eluted in slightly alkaline buffer.

6.3.4. Methylation-specific PCR

Methylation-specific PCR (MS-PCR) was carried out using two primer sets targeting the rat SOD2 promoter and bisulfite-converted DNA derived from each rat. Each MS-PCR reaction used ZymoTaq™ PreMix, 0.3 µM forward and reverse primers, approximately 50 ng of bisulfite converted DNA and nuclease-free water. ZymoTaq™ PreMix contains a hot start DNA polymerase specifically designed for the amplification of bisulfite-treated DNA (which can be fragmented and somewhat degraded) as well as a reaction buffer and dNTP mix. The PCR conditions for both primer sets used are tabulated below;

Table 5. MS-PCR cycling conditions.

Step	Temperature (˚C)	Duration (s)	Number of cycles
Initial denaturation	95	120	1
Denaturation	95	30	35
Annealing	50	30	35
Extension	72	40	35
Final extension	72	120	1

The successful amplification of each DNA target was confirmed with gel electrophoresis.

6.3.5. DNA cloning

Plasmid ligation

The DNA amplicons generated through MS-PCR were purified using the GeneJET PCR Purification Kit (Thermo Scientific), according to manufacturer's instructions. Following purification, DNA amplicons were ligated into the pGEM®-T Easy Vector (according to manufacturer's instructions) in a 1:3 ratio of vector to insert with T4 DNA Ligase, Rapid Ligation Buffer (Promega) and nuclease-free water. The solution was incubated for 1 to 3 hours at room temperature.

Bacterial transformation

The ligation mix was then incubated with JM109 Mix & Go Z-Competent™ *E. coli* Cells (Zymo Research), in a ratio of not more than 10 % of the final solution and streak plated onto LB agar plates that had been supplemented with 100 µg/ml Ampicillin, 0.1 mM IPTG and 0.003 % X-gal in DMF. The plates were incubated at 37 ˚C overnight, after which 2 to 3 white colonies from each transformation were selected for overnight liquid culture.

Plasmid purification and digestion

Plasmid DNA was isolated from the bacterial culture using the GeneJET Plasmid Miniprep Kit (Thermo Scientific) and quantified on a NanoDrop-1000 spectrophotometer. To ensure that each plasmid isolation contained the expected insert, plasmids were incubated with the *EcoRI* digestive enzyme and buffer (Thermo Scientific) for 1.5 hours. Digestion with *EcoRI* effectively excises the insert, creating two separate fragments that can be assessed for bp length using gel electrophoresis.

6.3.6. Sequencing and analysis

DNA fragments were sequenced by Inqaba Biotech using an ABI 3130XL sequencer and the Geospiza Finch Suite. Sequences were analyzed using FinchTV and then aligned to the expected target sequences using EMBOSS Needle (http://www.ebi.ac.uk/Tools/psa/emboss_needle/). For each category (young brain tissue and old brain tissue), 3 biological and 3 technical repeats were sequenced. The level of methylation in each DNA fragment sequenced was quantified as the amount of unconverted cytosine found in the final DNA product. The level of methylation of the two SOD2 promoter regions was compared between brain tissue of young and old rats.

7. RESULTS

7.1. GENE ANNOTATION ELUCIDATES THE PUTATIVE TRANSCRIPTIONAL AND EPIGENETIC REGULATORY SITES IN THE RAT SOD2 GENE PROMOTER

7.1.1. Basic SOD2 gene annotation illustrating conservation and GC frequency

The UCSC genome and WashU EpiGenome browsers revealed similar annotations for the rat SOD2 gene. The gene is located on chromosome 1, band q11. It consists of 5 exons and 4 introns and shows high levels of conservation across species in all exonic regions (Figure 1). Another highly conserved region is the CpG island that spans the upstream promoter region and continues into intron 2. (Figure 1). It follows that this region shows significantly high GC content. An enlarged version of Figure 1 can be found in appendix A (Figure A1).



Figure 1. Rat SOD2 promoter annotation illustrating species conservation and GC frequency. A) A region of the rat SOD2 gene as illustrated by the UCSC Genome Browser. The image depicts the gene CpG island shown as a green band, as well as exon 1 and 2. Other features illustrated are the high GC content and the high sequence conservation across 5 species. B) The complete rat SOD2 gene as illustrated by the WashU EpiGenome Browser. The gene is shown in the 3' to 5' direction. The CpG is shown as a green band, exons are shown as blue bands.

7.1.2. PATCH analysis reveals putative transcriptional binding sites in the SOD2 promoter

The PATCH analysis results generated for the 3' promoter region of the rat SOD2 gene corroborated with the published annotations of the SOD2 human and mouse genes, suggesting the presence of binding sites for the transcription factors NF-Kβ, NF-1, C/EBP, AP-1, AP-2 and Sp1 in the region approximately -500 bp upstream from the transcription start site.

7.1.3. Comprehensive SOD2 promoter annotation

The combined results of both singular gene annotations, the PATCH analysis and the manual promoter sequence comparisons were used to comprehensively annotate the rat SOD2 gene promoter with regards to its putative transcriptionally and epigenetically regulated elements (Figure 2). The image clearly illustrates a region beginning approximately -500 bp upstream of the transcription start site continuing into the first exon that contains a number of putative regulatory sites including binding sites for AP-2 and Sp1. Additionally, it demonstrates that this region is located within the promoter CpG island and subsequently has a high GC frequency. The putative structure of the rat SOD2 gene promoter shows similarity to that of the human and mouse genes. An enlarged version of Figure 2 can be found in appendix A (Figure A2).

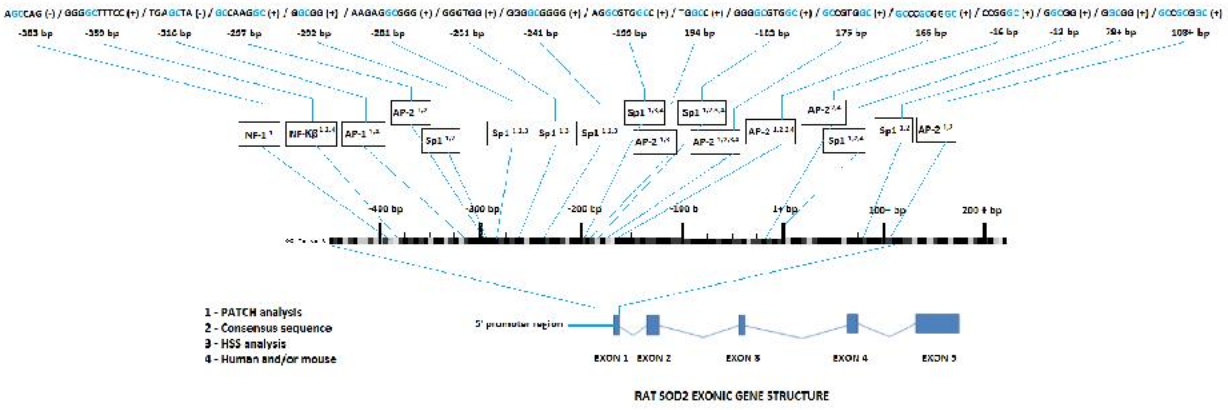


Figure 2. Comprehensive putative annotation of the rat SOD2 gene promoter region. Each annotation is based on more than one source, as indicated by the key. The figure illustrates a region of the 5' promoter and the putative binding sites located within it. The sequence of each binding site and its location are shown in relation to the transcription start site, 1+. The GC dinucleotides in each sequence are shown in blue font. Binding sites for NF-1, NFKβ and AP-1 are located -400 to -300 bp of the TSS, while multiple binding sites for AP-2 and Sp1 are distributed between -300 and 100+ bp of the TSS.

Each annotation was predicted using the above-mentioned accumulative data. The key provides information on the criteria that was used to annotate each binding site. The putative binding sites that are labelled with superscripts 1,2,3,4 were predicted by the PATCH analysis, showed 100 %

homology to the transcription factor binding site consensus sequence, were located within a hypersensitivity-site and showed a similar special arrangement to the homologous human and/or mouse SOD2 gene promoter region, respectively.

7.2. RT-PCR REVEALS AN INCREASE IN SOD2 EXPRESSION IN AGING LIVER AND A DECREASE IN SOD2 EXPRESSION IN AGING BRAIN

7.2.1. Confirmation of extracted RNA quality

All RNA samples used for cDNA synthesis and subsequently for RT-PCR had a concentration above 100 ng/µl and 280/260 and 230/260 ratios of between 1.8 and 2.2. Images of RNA samples extracted from the liver and brain of 6 rats (3 young and 3 old) obtained through gel electrophoresis are shown below (Figure 3). Images were inspected for the presence of two clear bands depicting the 28S and 18S RNA, the absence of genomic DNA contamination and significant degradation (indicated by smearing). The extracted RNA met all of the above criteria and was thus confirmed to be of good quality.

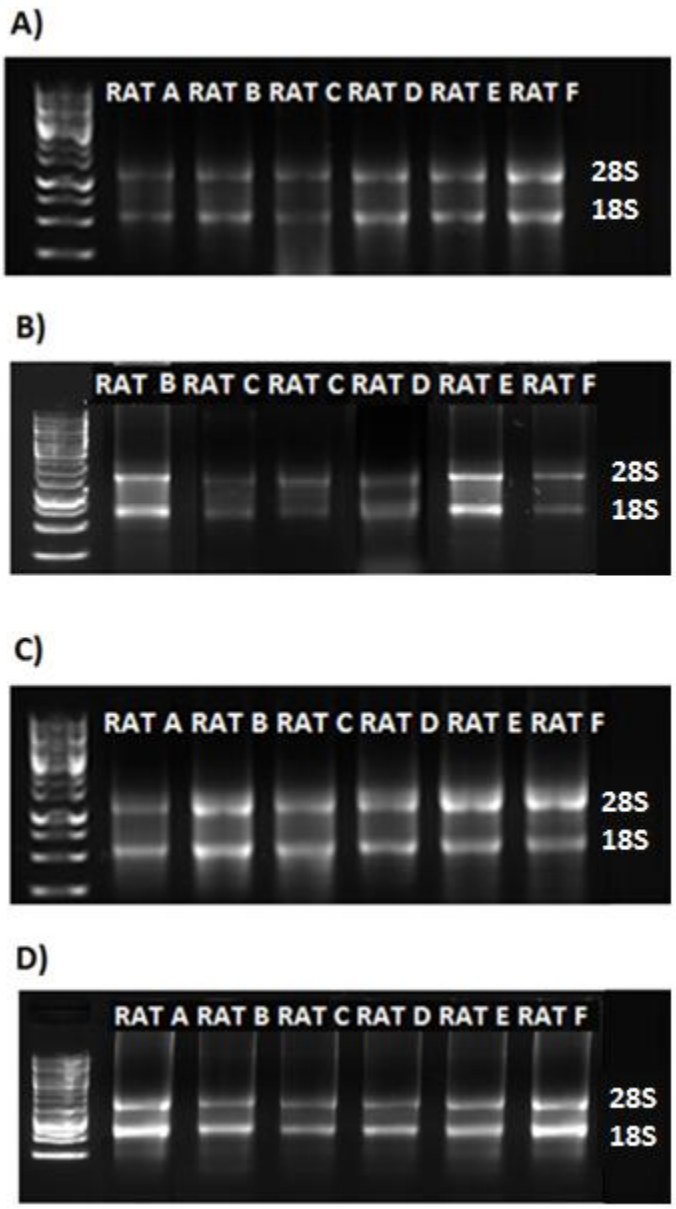


Figure 3. Gel electrophoresis images of extracted total RNA. Rats A, C and D were classified as "old" while rats B, E and F were "young". A total of 1 to 3 separate RNA samples were collected from the liver or brain tissue of each rat. The GeneRuler 1kb ladder was used with a molecular weight range of 250 bp to 10000 bp. A) and B) independently extracted RNA from brain tissue of each rat. C) and D) independently extracted RNA from liver tissue of each rat. RNA is confirmed to be of good quality due to the presence of two bright 18S and 28S bands and absence of smearing and contamination.

7.2.2. Melting curve analysis reveals target specificity for all genes

The primer sets used to detect mRNA transcripts for SOD2, CCT4, RAB11B and RPN1 were found to be specific for their intended targets. This was indicated by the presence of a single, narrow peak. The relative height of each curve indicated that the amplification reactions were efficient. Additionally, all four primer sets annealed successfully at 60 ˚C, allowing for the standardization of PCR cycling conditions for all RT-PCR experiments run. These features are depicted by the melting curves shown in Figures 4 to 7.

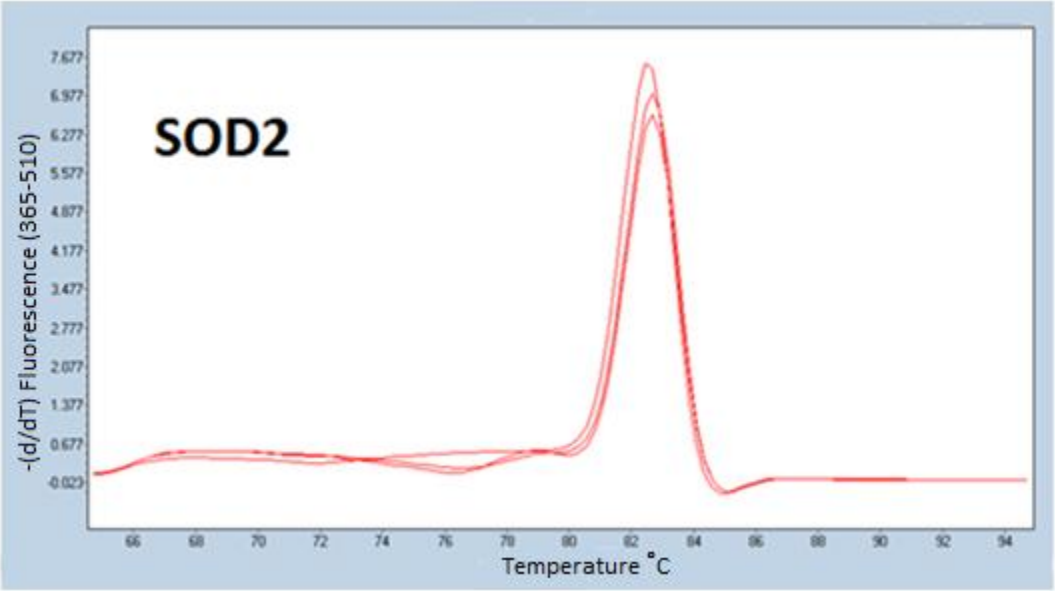


Figure 4. Melting curve of SOD2, confirming target specificity. The curve illustrates a single, sharp peak, indicating the absence of unexpected targets and the successful amplification of SOD2 mRNA.

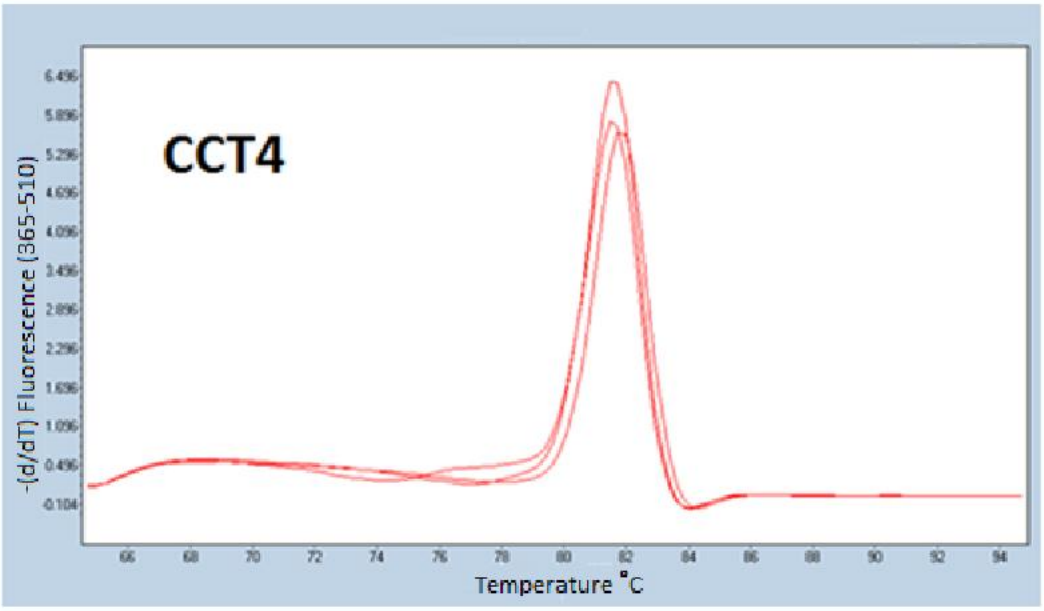


Figure 5. Melting curve of CCT4, confirming target specificity. The curve illustrates a single, sharp peak, indicating the absence of unexpected targets and the successful amplification of CCT4 mRNA.

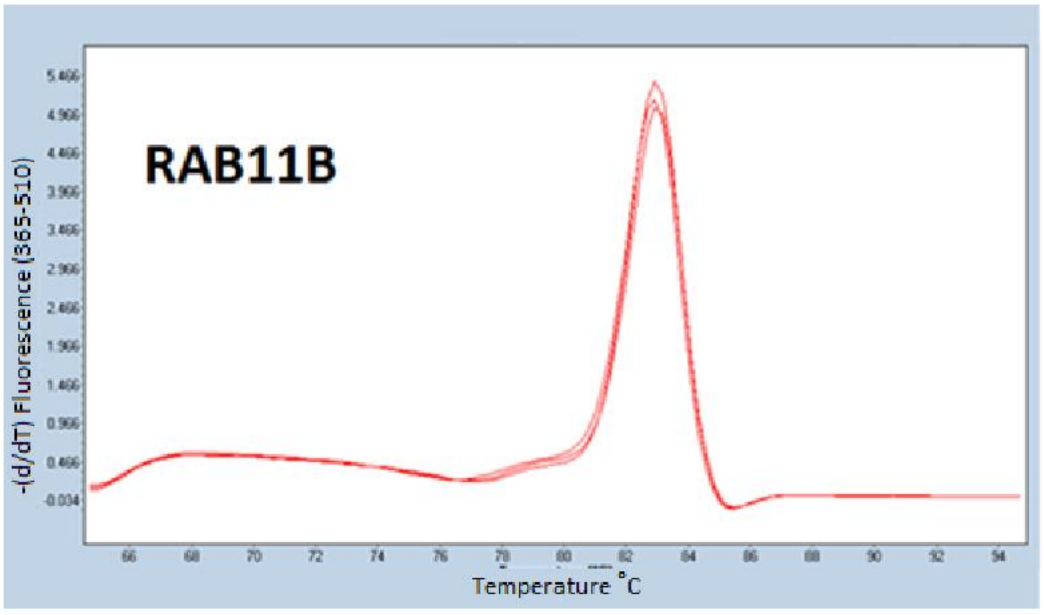


Figure 6. Melting curve of RAB11B, confirming target specificity. The curve illustrates a single, sharp peak, indicating the absence of unexpected targets and the successful amplification of RAB11B mRNA.

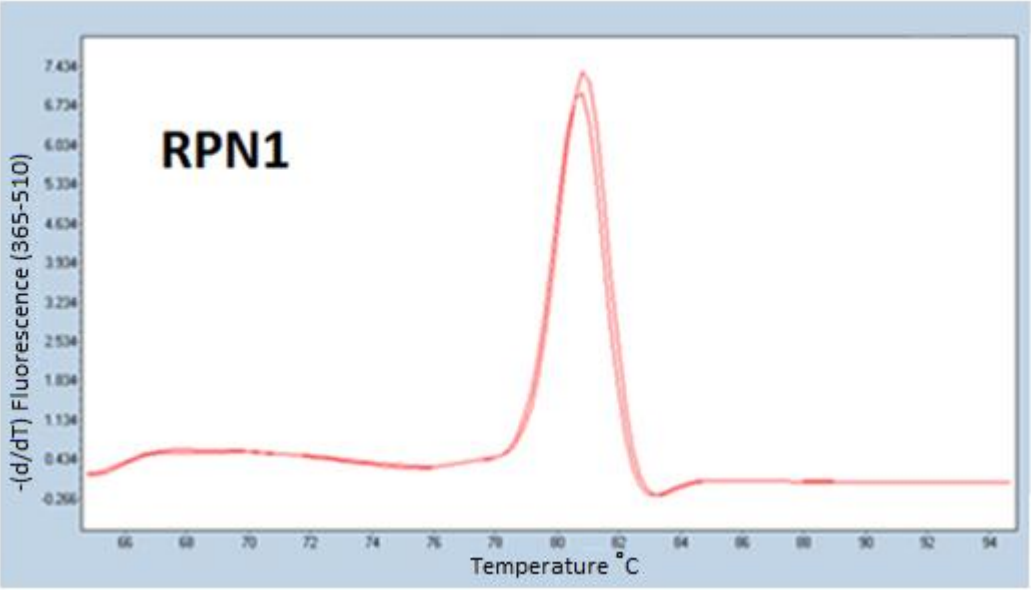


Figure 7. Melting curve of RPN1, confirming target specificity. The curve illustrates a single, sharp peak, indicating the absence of unexpected targets and the successful amplification of RPN1 mRNA.

7.2.3. Standard curve analysis confirms the efficiency, precision and sensitivity of RT-PCR gene amplification

The calibration curves generated through a series of RT-PCR reactions allowed for the assessment of the efficiency, sensitivity and precision of each gene amplification (Figures 8 to 11). The CP data values used to generate each curve are tabulated in appendix B, table B1. These values showed consistency (as indicated by the standard error bars) and indicated that the RT-PCR was sensitive over an approximate range of 0.01 ng to 100 ng of cDNA. The correlation coefficient calculated for each curve was no less than 0.98, where a correlation coefficient of 1 indicates a very strong negative correlation between the variables being assessed.

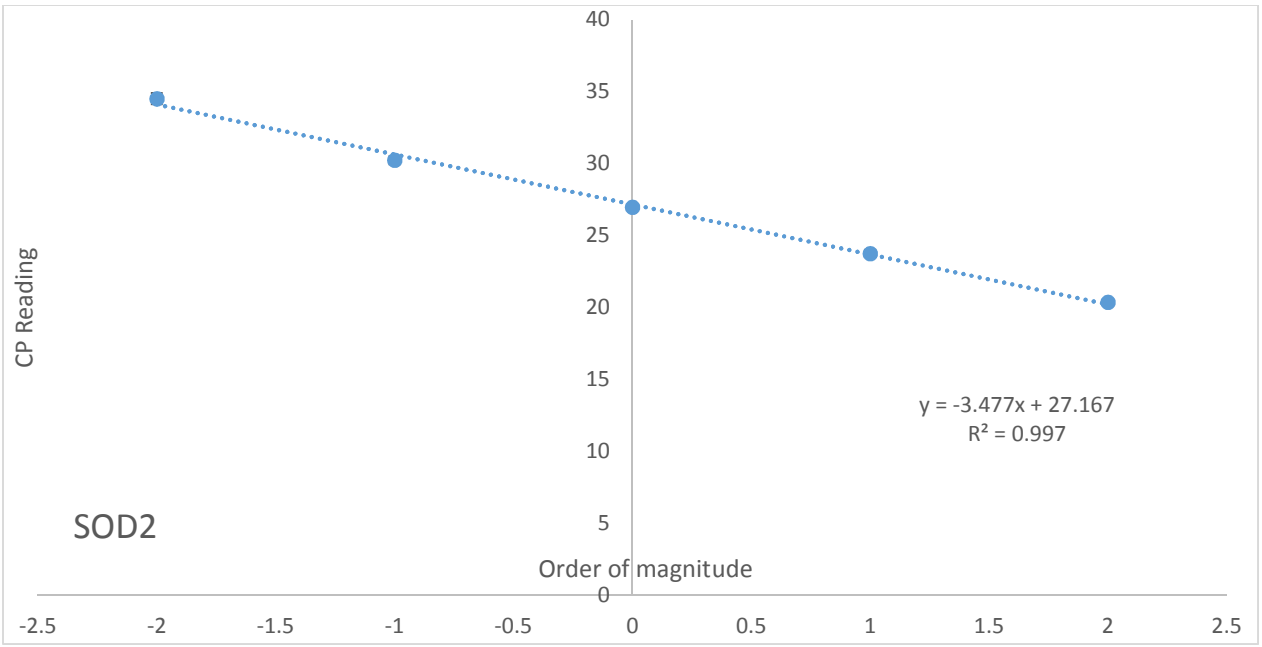


Figure 8. Standard curve for SOD2. The graph depicts the average CP value for each cDNA concentration. The standard curve generated illustrates a strong linear relationship between cDNA concentration and CP value (r^2 = 0.997) over 5 orders of magnitude.

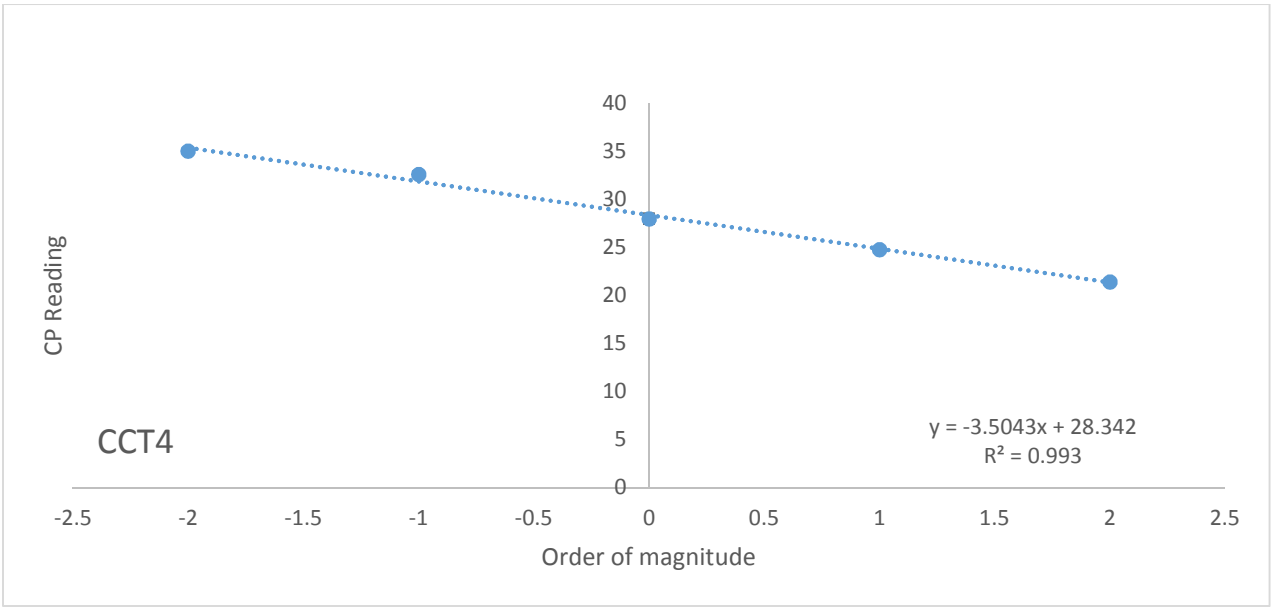


Figure 9. Standard curve for CCT4. The graph depicts the average CP value for each cDNA concentration. The standard curve generated illustrates a strong linear relationship between cDNA concentration and CP value (r^2 = 0.993) over 5 orders of magnitude.

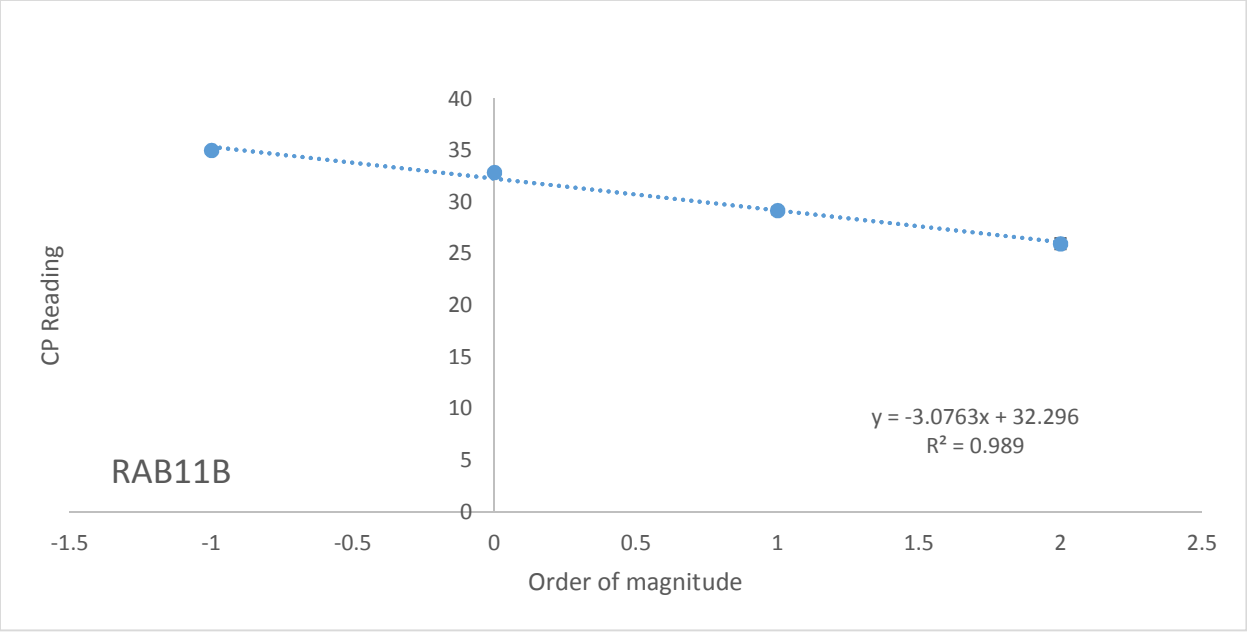


Figure 10. Standard curve for RAB11B. The graph depicts the average CP value for each cDNA concentration. The standard curve generated illustrates a strong linear relationship between cDNA concentration and CP value ($r^2 = 0.989$) over 4 orders of magnitude.

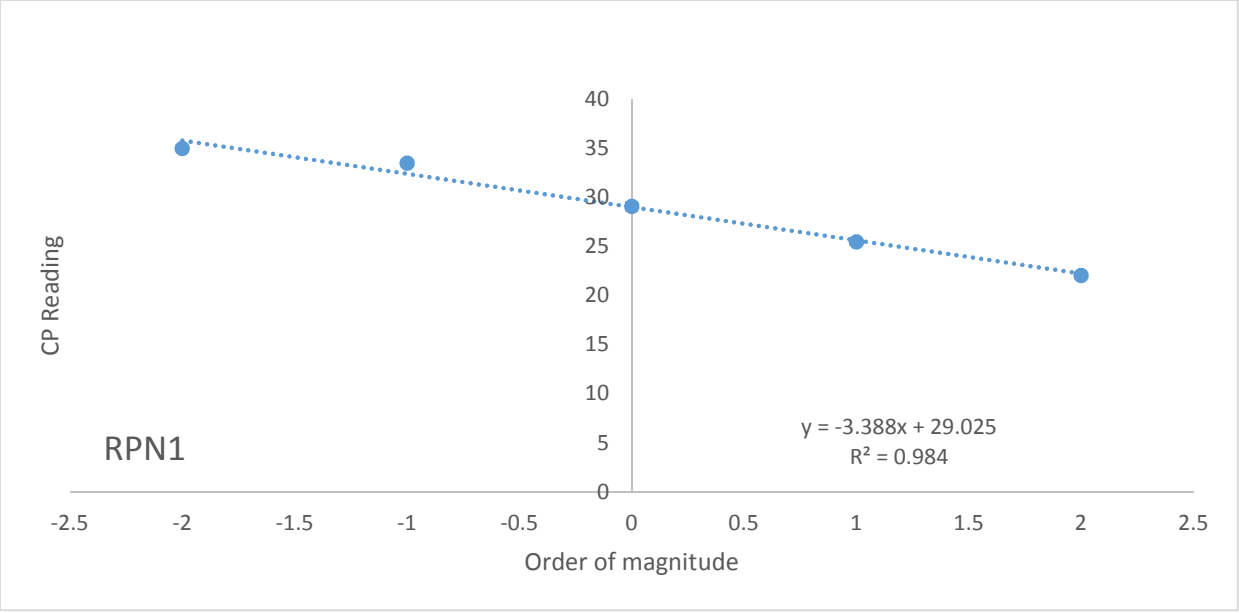


Figure 11. Standard curve for RPN1. The graph depicts the average CP value for each cDNA concentration. The standard curve generated illustrates a strong linear relationship between cDNA concentration and CP value ($r^2 = 0.984$) over 5 orders of magnitude.

The efficiency of all gene amplifications fell within the range of 1.8 to 2.2 (Table 1), where an efficiency of 2 is deemed ideal.

Table 6. Efficiency of gene amplification.

Gene	Efficiency
SOD2	1.94
CCT4	1.93
RAB11B	2.11
RPN1	1.97

7.2.4. Data normalization reveals a relative increase in SOD2 mRNA levels in aging rat liver and a relative decrease in aging rat brain

CP readings were obtained for SOD2 and three reference genes (in triplicate) using cDNA samples originating from liver and brain tissue of young and old rats. All raw data readings obtained from RT-PCR are tabulated in appendix B, table B2 and B3. All negative controls (both NRTC and NTC) showed insignificant levels of fluorescent signalling, showing CP values at least 3 cycles higher than the highest experimental value. Figure 12 summarizes the average normalized relative ratios of SOD2 mRNA found in young liver compared to old liver tissues. This data suggests that there is a relative increase in SOD2 mRNA levels in liver samples of old rats compared to those of young rats, however the relative difference in SOD2 mRNA levels between these two groups is not significant as illustrated by the standard error bars.

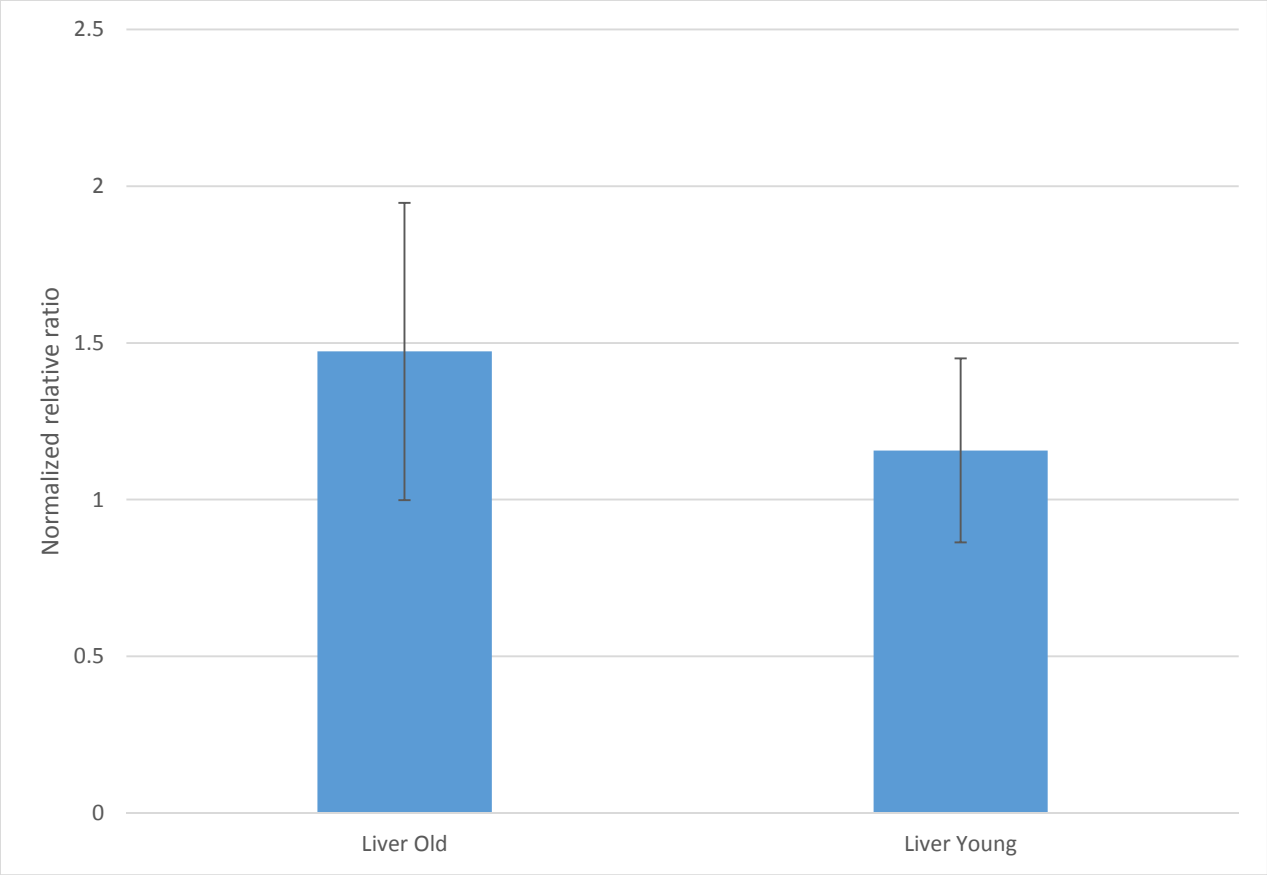


Figure 12. RT-PCR reveals increased SOD2 mRNA levels in tissues from old rat liver compared to young rat liver. The final average relative ratio in each group is an average of 3 values each obtained from a separate biological specimen. Each of these readings is based on CP values obtained in triplicate. The data suggests a relative increase in SOD2 mRNA levels in old liver tissue compared to young liver tissue, however this is not significant according to the standard error calculations.

Figure 13 illustrates the average normalized relative ratios of SOD2 mRNA found in young brain compared to old brain tissues. This data suggests that there is a relative decrease in SOD2 mRNA levels in brain samples of old rats compared to those of young rats, however the relative difference in SOD2 mRNA levels between these two groups is not significant as illustrated by the standard error bars.

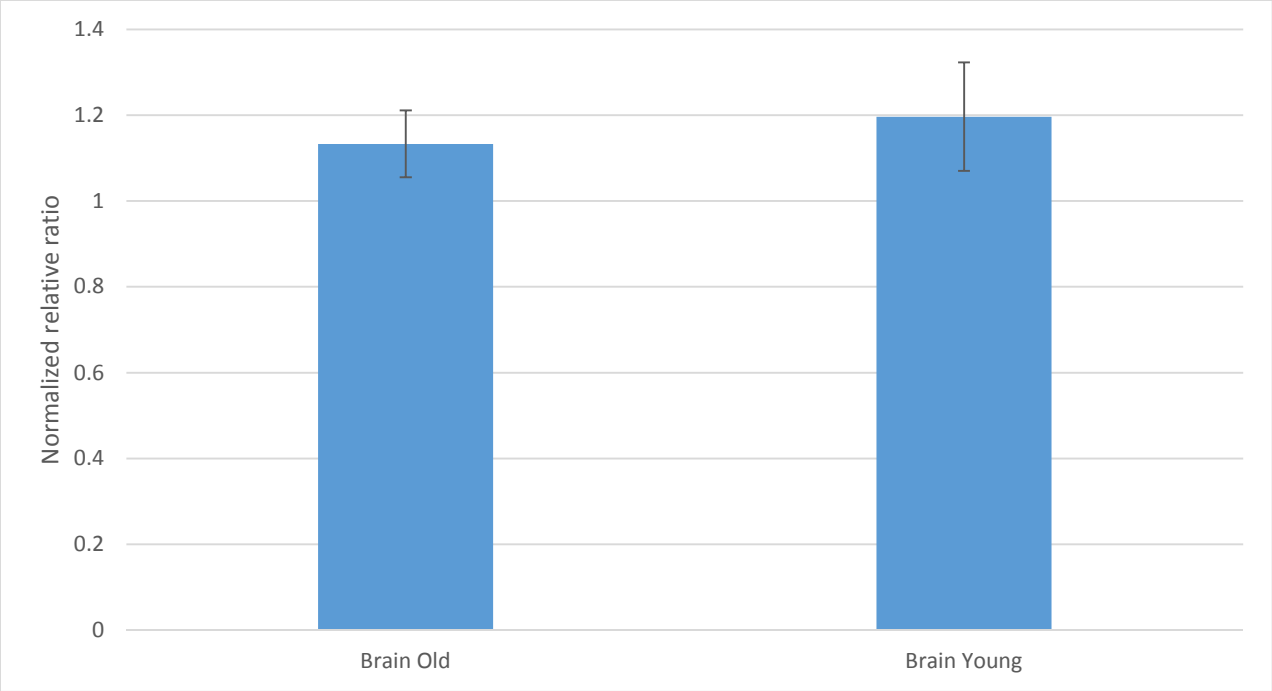


Figure 13. RT-PCR reveals decreased SOD2 mRNA levels in tissues from old rat brain compared to young rat brain. The final average relative ratio in each group is an average of 6 values each obtained from a separate biological specimen. Each of these readings is based on CP values obtained in triplicate. The data suggests a relative decrease in SOD2 mRNA levels in old brain tissue compared to young brain tissue, however this is not significant according to the standard error calculations.

7.2.5. Statistical analysis reveals that differences in SOD2 mRNA levels in young and old rat tissue are insignificant

The t-statistics for relative SOD2 mRNA levels in liver and brain tissues of young and old rats were calculated and the P(T<=t) two-tail values were assessed (Tables 5 and 6).

Table 7. t-Test for liver RT-PCR data confirms that differences in mRNA levels are statistically insignificant.

	Liver Old	*Liver Young*
Mean	1.47	1.16
Variance	1.01	0.39
Observations	3.00	3.00
Pooled Variance	0.70	
Hypothesized Mean Difference	0	
df	4.00	
t Stat	0.46	
P(T<=t) one-tail	0.33	
t Critical one-tail	2.13	
P(T<=t) two-tail	0.67	
t Critical two-tail	2.78	

Table 8. t-Test for brain RT-PCR data confirms that differences in mRNA levels are statistically insignificant.

	Brain Old	*Brain Young*
Mean	1.08	1.17
Variance	0.04	0.11
Observations	6.00	6.00
Pooled Variance	0.08	
Hypothesized Mean Difference	0	
df	10.00	
t Stat	-0.60	
P(T<=t) one-tail	0.28	
t Critical one-tail	1.81	
P(T<=t) two-tail	0.56	
t Critical two-tail	2.23	

The P(T<=t) two-tail values for both rat liver and brain RT-PCR data were greater than 0.05, confirming that there was no statistically significant difference between the young and old groups.

7.3. A METHYLATION ASSAY REVEALS THAT THE RAT SOD2 PROMOTER REMAINS LARGELY UNMETHYLATED WITH AGING

7.3.1. Confirmation of extracted DNA quality

All DNA samples used in bisulfite conversion and subsequently for MS-PCR had a concentration above 100 ng/µl and 280/260 and 230/260 ratios of between 1.8 and 2.2. Images of DNA samples extracted from the brain of 6 rats (3 young and 3 old) obtained through gel electrophoresis are shown below (Figure 14). Images were inspected for the presence of a predominant band greater than 10000 bp in size depicting intact genomic DNA, the absence of RNA contamination and significant degradation (indicated by smearing). The extracted DNA met all of the above criteria and was thus confirmed to be of good quality.

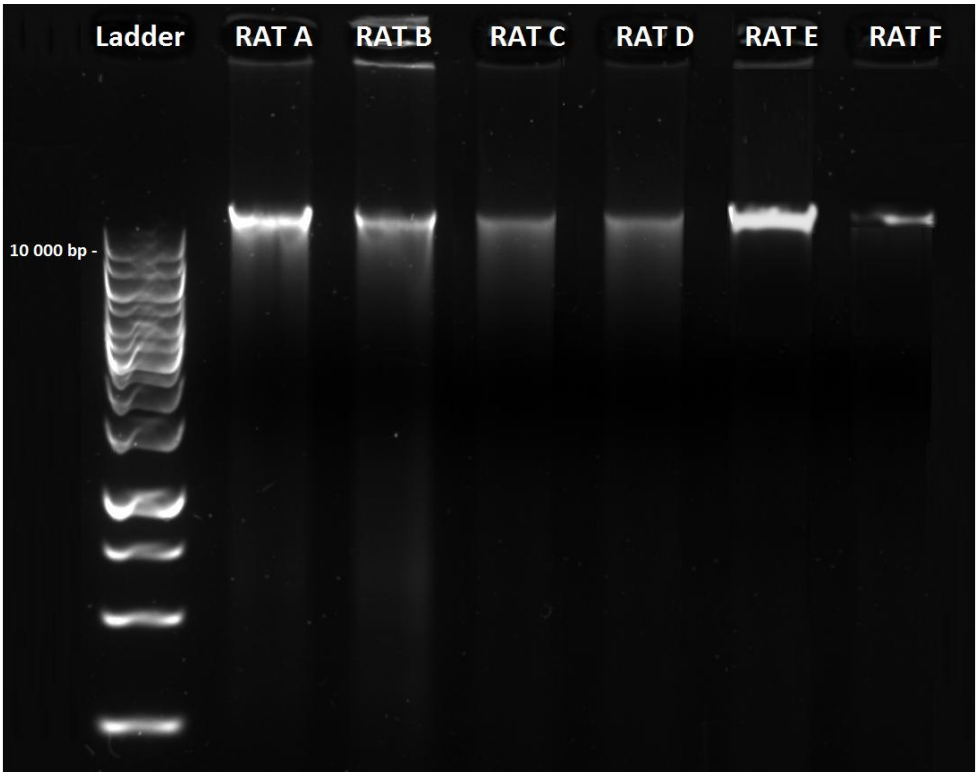


Figure 14. Gel electrophoresis image of extracted whole genomic DNA. DNA was inspected for integrity and purity using gel electrophoresis. Rats A, C and D were classified as "old" while rats B, E and F were "young". The GeneRuler 1kb ladder was used with a molecular weight range of 250 bp to 10000 bp. DNA is confirmed to be of good quality due to the presence of a DNA band greater than 10000 bp in size and the absence of smearing and contamination.

7.3.2. Confirmation of successful bisulfite conversion and Methylation-specific PCR

Primers designed to target two different regions of the rat SOD2 promoter region were found to be specific and successfully amplified each target amplicon (Figure 15). This also confirmed the success of bisulfite conversion, as the primers were designed to specifically target bisulfite converted DNA only. Each amplicon (region 1A and region 1D) was amplified using bisulfite converted DNA originating from the brain tissue of each rat (A to F).

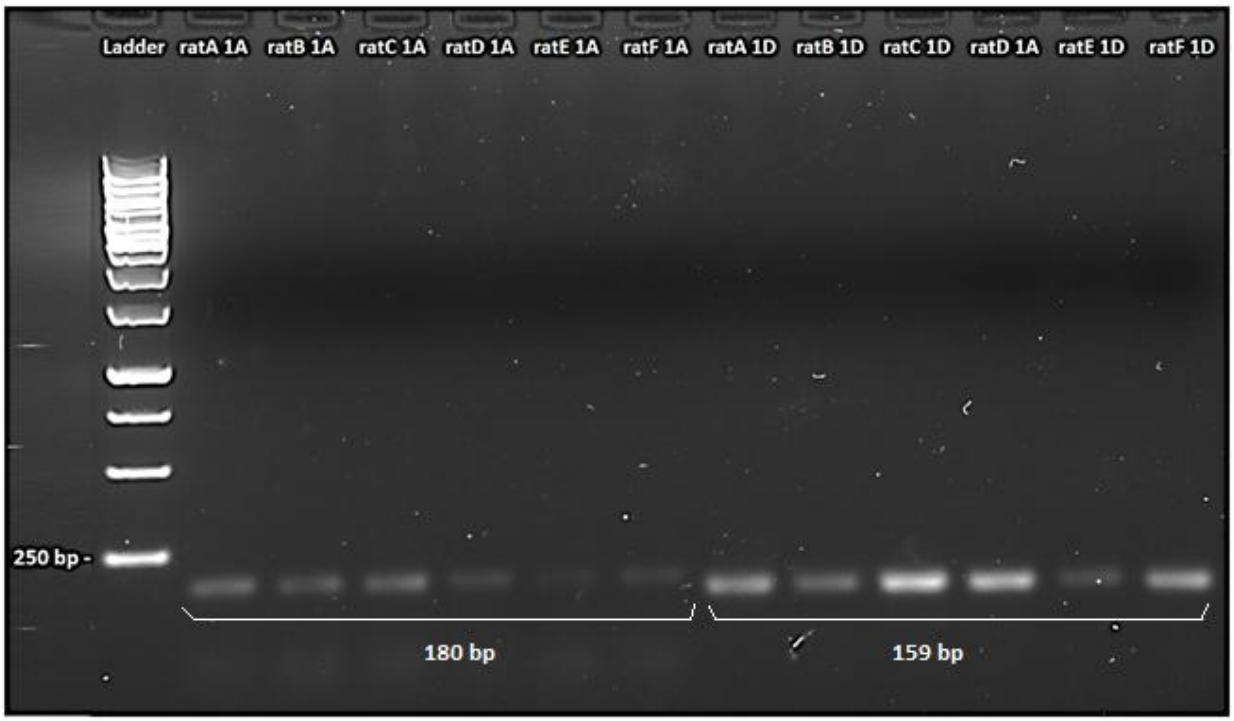


Figure 15. Successful MS-PCR amplification using primers for rat SOD2 promoter region 1A and 1D. The GeneRuler 1kb ladder was used with a molecular weight range of 250 bp to 10000 bp. The amplicon 1A is 180 bp in size while the amplicon 1D is 159 bp in size.

7.3.3. Confirmation of successful DNA cloning

Blue/white screening of each streak-plated bacterial transformation partially confirmed the success of ligation and transformation of each amplicon. This was further validated by the enzyme digestion of each isolated plasmid sample. Gel electrophoresis images of enzyme digested recombinant plasmids containing insert 1A and insert 1D can be seen in Figure 16.

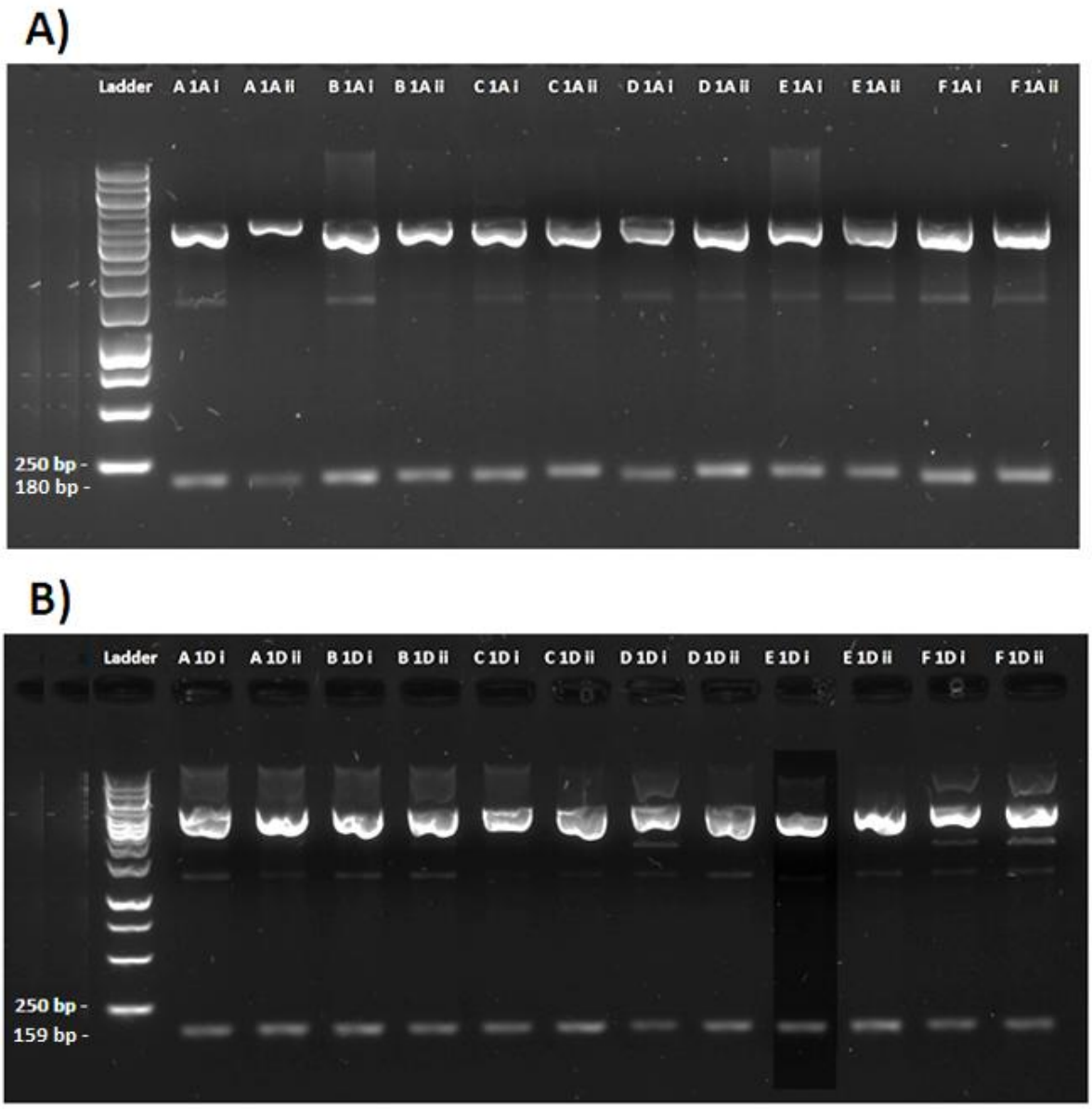


Figure 16. Enzyme digestions of recombinant plasmid samples indicate successful DNA cloning. Plasmids were isolated from two separate colonies. The GeneRuler 1kb ladder was used with a molecular weight range of 250 bp to 10000 bp. A) The insertion of amplicon 1A was confirmed by the presence of a band at approximately 180 bp. B) The insertion of amplicon 1D was confirmed by the presence of a band at approximately 159 bp.

7.3.4. Sequencing and analysis reveals that the rat SOD2 promoter region remains largely unmethylated with aging

For each amplicon originating from each rat, plasmid DNA from 2 to 3 colonies was sequenced and analyzed. The sequences were grouped into two categories, those originating from old brain tissue and those originating from young brain tissue. The multiple sequence alignments of each group and the unconverted amplicon (1A or 1D) are illustrated in Figures 17 and 18, respectively. Enlarged versions of Figure 17 and 18 can be found in appendix A as Figures A3 and A4.

The sequencing results show that in region 1A, 100 % of cytosine residues in both promoter regions have been converted into uracil and subsequently thymine, therefore there is 0 % methylation in DNA amplicons derived from old and young brain tissues.

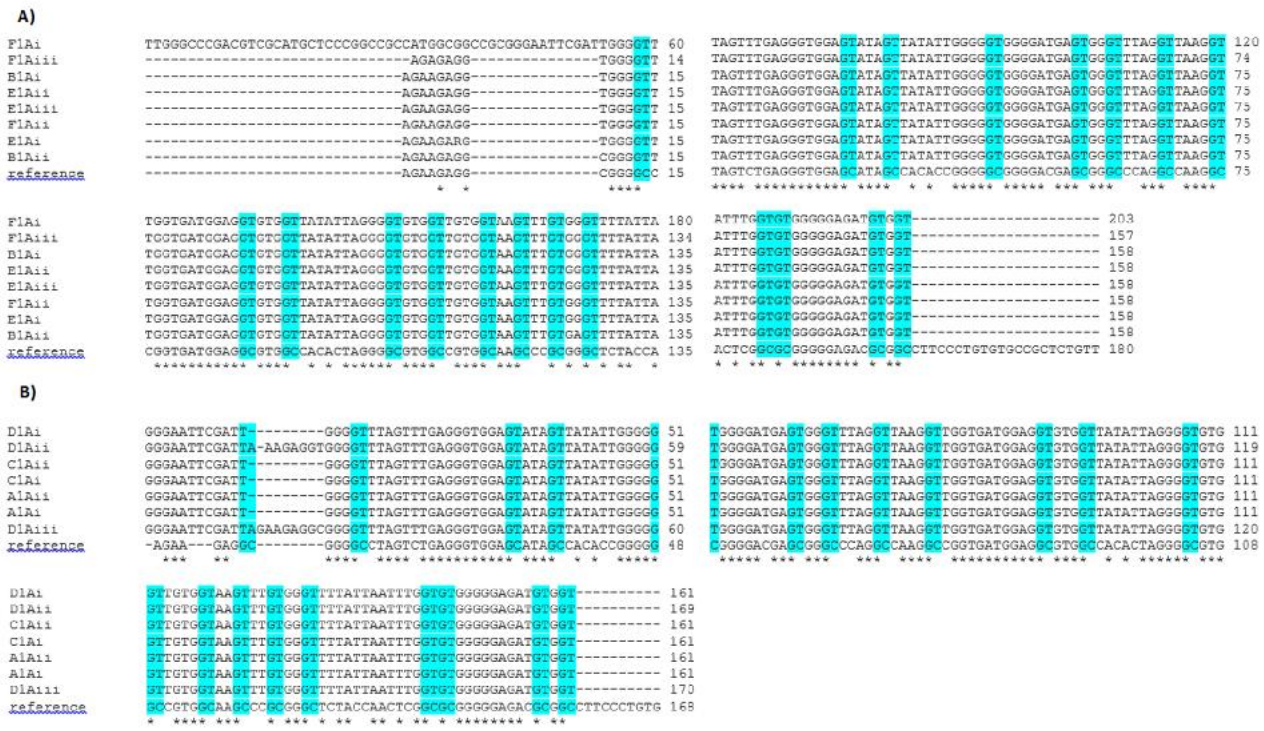


Figure 17. Multiple sequence alignment of rat SOD2 promoter region 1A and the unconverted DNA sequence illustrates that the rat SOD2 promoter remains largely unmethylated in aging brain tissue. Converted CpG dinucleotides are highlighted in blue. A) All sequences originate from young brain tissue. B) All sequences originate from old brain tissue.

In region 1D isolated from young brain tissue (Figure 18 A) 1 cytosine residue appears to be methylated and is located in the 22nd CpG dinucleotide highlighted. This methylation is present in 1 out of 7 amplicons sequenced. In region 1D isolated from old brain tissue (Figure 18 B) 1 cytosine residue appears to be methylated and is located in the 2nd CpG dinucleotide highlighted. This methylation is present in 2 out of 8 amplicons sequenced.

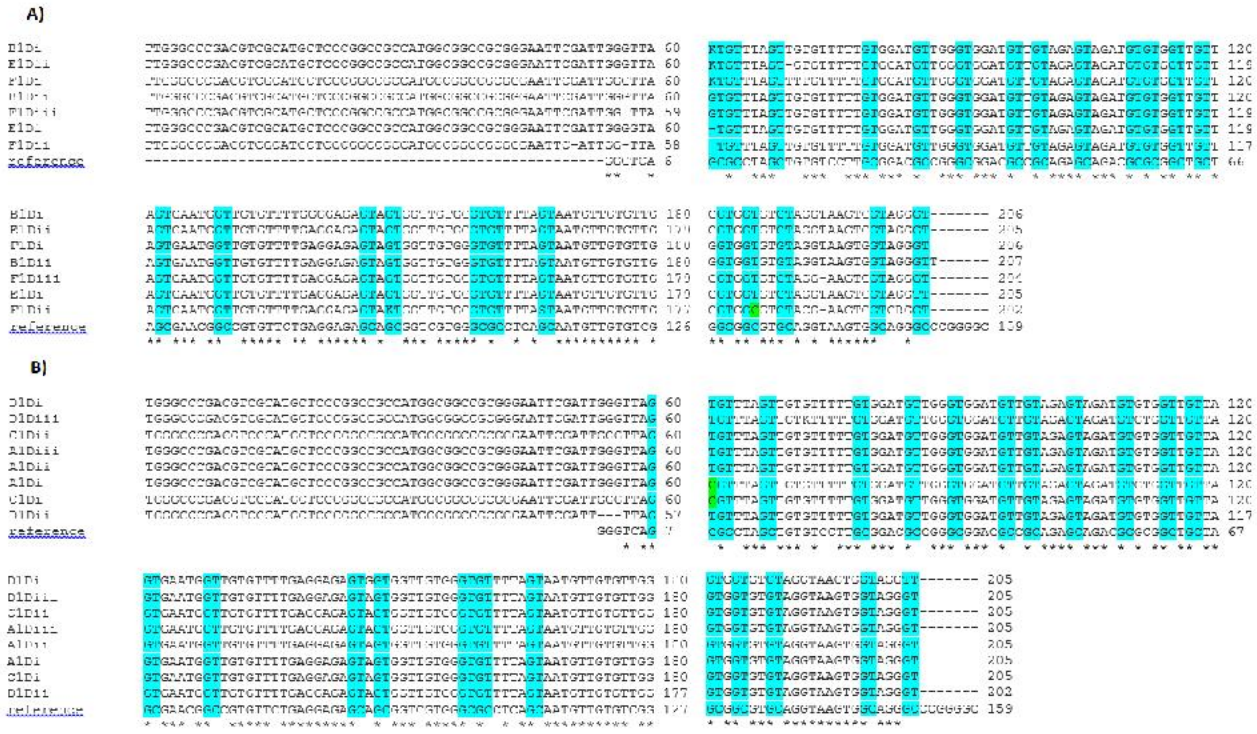


Figure 18. Multiple sequence alignment of rat SOD2 promoter region 1D and the unconverted DNA sequence illustrates that the rat SOD2 promoter remains largely unmethylated in aging brain tissue. Converted CpG dinucleotides are highlighted in blue, methylated cytosines are highlighted in green. A) All sequences originate from young brain tissue. B) All sequences originate from old brain tissue.

8. DISCUSSION

8.1. MNSOD ACTIVITY AND REGULATION CHANGES WITH AGING

Manganese superoxide dismutase (MnSOD) has been identified as a critical factor involved in the regulation of aging and age-related disease (Warner, 1994; Rosen et al., 1993; Velarde et al., 2012). In general terms, MnSOD neutralizes toxic superoxide within the mitochondria of the cell, thereby preventing downstream oxidative damage to the mitochondrion itself as well as to other cellular components (Miao & Clair, 2009). As it functions exclusively in the mitochondria, the predominate site of oxygen metabolism and ROS production, it is the most vital of the SOD enzymes. This has been demonstrated in transgenic mouse studies where homozygous MnSOD-deficient mice exhibit neonatal lethality (Huang et al., 1997) and in mice heterozygous for MnSOD that are more susceptible to oxidative stress and have reduced mitochondrial function (Kokoszka et al., 2001; Velarde et al., 2012). Reduction of mitochondrial capacity and the accumulation of oxidative damage in the cells of old mammals are fundamental concepts in the free radical theory of aging, however to date, the exact cause of these phenomena has not been conclusively elucidated (Alexeyev, Doux & Wilson, 2004; Liochev, 2013). A promising theory in this regard posits that major features of the aging phenotype can be attributed to an overall reduction in the cell's antioxidant defenses, more specifically, a reduction in the activity and prevalence of key antioxidant enzymes.

Numerous correlation studies in human and rodent models have been performed to investigate the activity of major antioxidant enzymes, including MnSOD in the aging context. These studies demonstrate that changes in MnSOD activity with aging are highly tissue-specific and the trends elucidated are not altogether consistent across studies. (Cand and Verdetti, 1989; Navarro and Boveris, 2004; Navarro et al., 2003; Tian, Cai & Wei, 1998). For simplicity, the studies used in this comparison are restricted to those investigating MnSOD activity in the brain and liver tissues of rodents. Cand and Verdetti (1989) demonstrated an age-related decrease in MnSOD activity in liver homogenate of Wistar rats but consistent levels of MnSOD activity in brain homogenate.

MnSOD activity was measured through an inhibition assay. Tian, Cai & Wei (1998) also made use of an inhibition assay and found no significant change in the activity of MnSOD in brain and liver homogenates of Fischer rats with aging, but did find a decrease in MnSOD activity in liver mitochondria. Navarro and Boveris (2004) and Navarro et al. (2003) made use of the adrenochrome assay and measured MnSOD activity in liver and brain mitochondria and liver and brain tissue homogenate of CD-1 mice and Wistar rats, respectively. Their research demonstrated a unanimous age-related decrease in MnSOD activity across tissues and rodents.

Discrepancies in the results of these studies may be a result of the different assay methods used, strain and ages of rats used and whether MnSOD activity was measured in whole tissue homogenate or isolated mitochondria. However, in light of the fact that the most recent investigations by Navarro et al. (2003) and Navarro and Boveris (2004) used larger sample groups (8 to 20 per group) and found consistent results across mice and rats and in tissue homogenate and isolated mitochondria, it can be assumed that these are reliable findings and that MnSOD activity may in fact decrease as a function of age in liver and brain tissue. This reduction in enzyme activity was paralleled by a number of other enzymes critical for mitochondrial function, including mitochondrial nitric oxide synthase, complex I, and complex IV. It was also associated with an increased content of oxidation products, thiobarbituric acid-reactive substances and protein carbonyls as well as increased mitochondrial fragility, volume and water permeability (Navarro & Boveris, 2004). The significant decrease in the activity of critical mitochondrial enzymes and overall mitochondrial function and the concurrent increase in oxidative damage demonstrated in this study lends validity to the theory that key features of the aging cell may be a result of a degenerative antioxidant defense system.

A reduction in overall enzyme activity with aging seen in studies like that of Navarro and Boveris (2004) could be affected through a number of possible mechanisms at the transcriptional or translation levels. These may include; a) poor maintenance and higher turnover of MnSOD protein with aging, b) reduced levels of MnSOD protein synthesis, c) increased turnover of MnSOD mRNA, or d) reduced transcription of the MnSOD gene.

The turnover of MnSOD mRNA as well as the level of MnSOD protein synthesis could be influenced by general mechanisms of post-transcriptional regulation including mRNA processing and export as well as microRNA modulation and mRNA binding proteins (Miao & St Clair, 2009). Both the basal and stimulus-induced post-transcriptional regulation of MnSOD is determined by a ~280-nucleotide fragment located in the mRNA coding region which determines mRNA stability (Davis, Monnier & Nick, 2001). Additional post-transcriptional control elements include an Alu-like element in the MnSOD 3' untranslated region (UTR) that may be a putative target for microRNA (Stuart et al., 2000; Smalheiser & Torvik, 2006) and a redox-sensitive MnSOD RNA-binding protein that appears to have both positive and negative effects on the translation efficiency of MnSOD (Chung, Wright & Clerch, 1998; Knirsch & Clerch, 2000). Although any one of these mechanisms could potentially account for a decrease in MnSOD activity with aging, their function in the regulation of MnSOD in the aging context has not yet been explored.

At the post-translational level, where the maintenance and turnover of MnSOD protein may affect its activity, a number of regulatory mechanisms exist for MnSOD. A study by Xu et al. (2006) investigated the sequence-specific tyrosine nitration of MnSOD in cardiovascular disease and aging. Tyrosine nitration is a marker of oxidative stress that can potentially alter the biological activity of the modified protein (Xu et al., 2006). Specifically, MnSOD, a protein that is nitrated in its active catalytic sites, is rendered inactive by the nitration of a single tyrosine (Xu et al., 2006). This research, corroborated by Loo et al. (2000) who also reported nitration and inhibition of MnSOD in vascular aging, demonstrated that MnSOD is particularly vulnerable to tyrosine-nitration in aging which lead to a reduction in enzymatic activity. Down-regulation of MnSOD activity due to what is essentially oxidative damage, suggests that the accumulation of oxidative stress in the aging cell is not initially a result of decreased antioxidant function but that decreased antioxidant function is actually initiated by oxidative damage. Although this theory is plausible, it is still unclear why oxidative damage begins to overwhelm the cell's formidable antioxidant defence system with age.

Another post-translational regulatory mechanism that may influence MnSOD activity with aging is the reversible acetylation of specific, evolutionarily conserved lysine residues in the MnSOD protein (Ozden et al., 2011; Tao et al., 2010). Lysine acetylation has recently emerged as an important post-translation modification in the regulation of mitochondrial proteins (Choudhary et al., 2009) as several proteomic surveys have revealed significantly high levels of acetylated proteins in the mitochondria (Kim et al., 2006).

Studies by Ozden et al. (2011) and Tao et al. (2010) have investigated the inverse relationship between MnSOD activity, MnSOD acetylation and levels of cellular SIRT3 (sirtuin 3) protein. Sirtuins are class III histone deactylases that have been implicated in aging and longevity in various models (Wood et al., 2004). These enzymes appear to function as fidelity proteins that alter the activity of downstream mitochondrial targets in response to oxidative stress (Choudhary, 2009). Tao et al. (2010) demonstrates a relationship between MnSOD activity and SIRT3, where the absence of SIRT3 in knockout mice leads to increased MnSOD acetylation and decreased MnSOD activity while the reintroduction of SIRT3 restores MnSOD activity. Additionally both Ozden et al. (2011) and Tao et al. (2010) confirm that SIRT3 interacts with MnSOD *in vitro*. As the sirtuin proteins have been implicated in lifespan and longevity it follows that post-translational regulation of MnSOD by SIRT3 may be a mechanism involved in the decreased levels of MnSOD seen in aging. This may be due to a down-regulation of SIRT3-mediated mitochondrial homeostasis as demonstrated by Brown et al. (2013) in hematopoietic stem cells.

According to these studies a decrease in SIRT3 regulation would lead to an overall increase in MnSOD acetylation and a subsequent decrease in MnSOD activity. Although down-regulation of MnSOD through this mechanism is possible, it is unclear what would trigger a progressive down-regulation in SIRT3 regulation initially. Therefore, it may be of more use to investigate key regulators of mitochondrial function in a context where the source of abnormal function can be identified.

Although the above-mentioned post-transcriptional and post-translational regulatory mechanisms are not restricted to MnSOD, they do not account for an overall decrease in the cell's defense against oxidative damage. Numerous proteins are implicated in this process, introducing enormous variety in the control elements that govern their eventual fate. It is therefore more likely that a generalized trend such as this is a result of a more common cellular mechanism. This is suggestive of regulation at the transcriptional level, where all genes are subject to the restrictions of chromatin structure.

A generalized mechanism of down-regulation at the level of gene transcription could account for the decreased activity seen in a number of antioxidant and mitochondrial enzymes with aging (Navarro and Boveris, 2004). As previously described, the activity of critical antioxidant enzymes in relation to aging has been assayed in various organisms as well as tissues, however the quantification of their specific mRNA species in this context has only been investigated in a limited number of studies. To date, work done to elucidate the trend, if any, that MnSOD expression shows with aging has proved to be inconsistent.

A study by Rao, Xia and Richardson (1990) investigated the effect of age on the expression of several antioxidant enzymes in rat brain, hepatocyte and kidney. This study demonstrated an age-related decrease in SOD and catalase mRNA in these tissues that paralleled a decrease in enzyme activity with aging. However SOD activity constituted both that for CuZnSOD and MnSOD, therefore the specific trend for each enzyme is indistinguishable. The levels of mRNA were determined using a dot blot analysis, an outdated technique that has now been surpassed by a number of more reliable techniques, including reverse transcription quantitative PCR. Four Wistar rats were used for each group, young (4 months) and old (24 months). A more recent study by Tsay et al. (2000) focused on the age-associated changes of superoxide dismutase and catalase activities in the rat brain. mRNA levels were assayed using a ribonuclease protection analysis and were found to be consistent with aging. This study used 3 Wistar rats per group at 1, 3, 6, 12, 18 and 21 months old.

Martin et al. (2002) made use of RT-PCR to investigate the effect of hypoxia/reoxygenation on mRNA expression of antioxidant enzymes in rat liver and kidneys. This study found a decrease in mRNA expression of all enzymes studied except for MnSOD in aging liver and a progressive decrease in all antioxidant enzymes in aged kidney tissue. Each age group, young (6 months) and old (22 - 25 months) was made up of 7 to 8 male Wistar rats.

In light of the inconsistent nature of the work performed to investigate a trend in mRNA levels of MnSOD and other enzymes in aging to date, it is possible that more reliable and reproducible work needs to be completed to this end. This research aimed to quantify and compare levels of SOD2 mRNA in extracts from young and old rat brain and liver tissue using the current gold-standard in mRNA quantification, reverse transcription quantitative PCR.

The current study investigated the SOD2 mRNA levels in brain and liver tissue homogenates of young (1 to 2 months) and old (15 to 19 months) Sprague Dawley rats. The RT-PCR results demonstrate a slight increase in SOD2 levels in older liver tissue (Figure 12), and a slight decrease in SOD2 levels in older brain tissue (Figure 13), however neither of these results are statistically significant according to the standard error calculations and t-test analyses (Tables 5 and 6). As a result this data can be interpreted in one of two ways; either the lack of a statistically significant difference between SOD2 mRNA levels in old and young rat tissues indicates that these mRNA levels remain relatively constant with age, or the trends illustrated by the results have some biological meaning, but a larger sample size is required to confirm them statistically. If the latter argument is considered, results of this study are contrary to that of Tsay et al. (2000) and consistent with that of Martin et al. (2002) who demonstrated consistent SOD2 mRNA levels in aging brain and increased SOD2 mRNA levels in aging liver tissue, respectively.

It is important to note that similar to studies assessing MnSOD activity, a number of technical considerations could influence the results of correlative study such as this. It appears that large variation exists in SOD2 mRNA levels between rats (appendix B, tables B2 and B3). Variation of this nature is often observed when many biological replicates are used in an effort to increase

the statistical significance of the results obtained, especially when the experimental differences being assessed may be subtle (Bustin et al., 2009). In this case sufficient numbers need to be included in order to allow for more subtle experimental differences to be elucidated (Bustin et al., 2009). For example, Martin et al. (2002) used up to 8 rats for each age group.

Another consideration is the comparable age groups of the rats classified as either “young” or “old”. The majority of studies investigating enzyme activity and or gene expression with aging used rats between 4 and 6 months of age in the young group and 21 to 24 months of age in the old group, whereas “young rats” included in this study were 1 to 2 months of age and “old” rats were 15 to 19 months of age. A study by Tian, Cai and Wei (1998) showed that rats at 1 month old showed the lowest activities of total SOD, MnSOD and CuZnSOD in all tissues, which may imply that that at this stage, the antioxidant defence system is not yet mature, or the antioxidant enzymes have not yet been adequately induced due to a lack of prooxidant exposure. If MnSOD levels are in fact significantly lower at this age, this may account for the very subtle decrease and actual increase seen in SOD2 mRNA levels of old brain and liver tissue, respectively, as opposed to a significant decrease in SOD2 mRNA levels expected for both aging tissues. Additionally, it is possible that the “old” rats in this study were not old enough to show significant differences in SOD2 mRNA levels compared to young rats. According to the results of Tsay et al. (2000), MnSOD levels only begin to decrease after 12 months in age and are lowest at 21 months. This suggests that the mRNA levels measured in 15 to 19 month old rats may still have been relatively high compared to other older (21 to 24 months) rats.

It is also important to note that MnSOD is susceptible to both basal and induced expression (Rogers et al., 2000) and regulation of these different types of expression occurs in different areas of the gene. Therefore, even though it would be more useful to ascertain the basal levels of MnSOD transcription with aging, we cannot exclude the levels of mRNA that have been induced by proinflammatory mediators, which will vary under different conditions. This would naturally increase variation between biological samples. Finally, it may be important to consider that the

rat brain has been shown to have region-specific antioxidant levels (Tsay et al., 2000) and that using unspecified brain regions might contribute to variation in mRNA levels measured.

In light of these considerations, further study would need to be implemented to conclusively delineate the pattern of SOD2 expression in the aging context. In order to achieve statistically significant results it may be useful to perform a power analysis to determine the number of samples necessary. It is also advisable to examine SOD2 mRNA levels at various ages to investigate the possibility of a two-part trend (initial MnSOD increase and then subsequent decrease later in life) as indicated by Tsay et al. (2000). Finally, it may be beneficial to ensure that rats included in the study are in excellent health and do not show any signs of biological variation in terms of inflammatory response or overexposure to oxidative stress.

The results of this study indicate that the age-related decrease in MnSOD activity demonstrated in studies by Navarro & Boveris (2004) and Navarro et al. (2003) may be a result of transcriptional down-regulation of SOD2 in brain tissue of rats. In order to explore potential epigenetic-induced down-regulation of the SOD2 gene in aging, this study quantified and compared promoter methylation of the SOD2 gene promoter in extracts from young and old rat brain tissue.

8.2. EPIGENETIC REGULATION OF MNSOD IN THE AGING CONTEXT

Transcriptional regulation is largely controlled by the transient state of the chromatin structure and subsequently by the epigenetic modifications that govern it. An epigenetic mechanism that has long been associated with age-related changes is DNA methylation, where CpG dinucleotides predominantly found in CpG islands have demonstrated abnormal patterns of methylation (Klose & Bird, 2006). As previously mentioned, the hypermethylation of gene promoters is a repressive epigenetic mechanism that has been implicated in cancer as well as aging. Various genes for tumour suppression, metabolism and DNA repair have demonstrated abnormal promoter methylation (Gentilini, et al., 2012; Winnefeld & Lyko, 2012). In addition to this, more general trends of 'epigenetic drift' have been revealed in association with aging, cancer and neurodegenerative disease, suggesting that this general loss of transcriptional control may be an implicative factor in aging and age-related disease (Gentilini, et al., 2012; Winnefeld & Lyko, 2012; Herman & Baylin, 2003; Ehrlich, 2002; Wang, Oelze, & Schumacher, 2008).

The MnSOD gene, SOD2, has a large CpG island that spans the promoter and extends into intron two (Wan et al., 1994; Ho, Howard & Crapo, 1991; Jones et al., 1995). This GC-rich region contains numerous transcriptional binding sites and has been found to be well conserved in human, rodents and other mammals. Although the human and mouse SOD2 gene promoter regions are well annotated, the rat promoter features are yet to be conclusively delineated. The human SOD2 gene has multiple binding sites for Sp1 and AP-2 as well as binding sites for NF-1, AP-1, C/EBP and NFKβ. The Sp1 and AP-2 binding sequences are found predominantly in the region -500 bp upstream to 100+ downstream of the transcription start site (TSS), occur in GC-rich "boxes" and are often overlapping (Xu, Porntadavity & St Clair, 2002). The NF-1, AP-1 and NFKβ binding sequences are less abundant, with binding sites for NFKβ and AP-1 being located approximately -2000 bp and -750 bp upstream of the TSS and binding sites for NFKβ, NF-1 and C/EBP being located in a region near the end of intron 2, referred to as the intronic enhancer (Miao & St. Clair, 2009).

The *in vivo* architecture of the rat SOD2 gene has been investigated using DNAse I- hypersensitive site analysis and dimethyl sulfate *in vivo* footprinting (Kuo et al., 1999). This study revealed 5 hypersensitive sites within the promoter region and 10 putative constitutive protein-DNA binding sites (Kuo et al., 1999). These sites are located in the region approximately -500 bp from the TSS and are able to bind Sp1. Additional work by Rodgers et al. (2000) has localized the rat SOD2 gene intronic enhancer to a 260 bp fragment in intron 2. This work and other research that refers to homologous binding sites in the rat promoter suggests that the rat SOD2 gene is transcriptionally regulated in a similar manner to the human gene, however the validity of these sites has not yet been confirmed and a comprehensive picture of the regulatory elements at the rat SOD2 promoter has not yet been established.

In order to address this apparent lack of cumulative information, the transcriptional and epigenetic elements in the rat SOD2 promoter were investigated by reviewing information obtained from the literature thus far and by providing additional insight through the use of appropriate bioinformatics tools. The accumulative data for the USCS/ EpiGenome browser annotations, the PATCH analysis as well as other comparisons performed (see methods and materials) demonstrates that the rat SOD2 promoter region contains putative binding sites for NF-1, NFKβ, AP-1 as well as numerous putative binding sites for the AP-2 and Sp1 transcription factors (Figure 2). These sites are concentrated in the region approximately -500 bp to 100+ bp of the TSS, with some Sp1 and AP-2 sites overlapping. The binding sequences for Sp1 and AP-2 are particularly GC-rich and each contain at least one CpG dinucleotide (excluding one Sp1 site). The AP-1, NF-1 and NFKβ binding sequences also contain at least one CpG dinucleotide each. This illustrates that similar to human and mouse, the rat SOD2 gene may be susceptible to regulation by a number of redox-related proteins through the mechanism of DNA-binding. As many of the putative transcription factor binding sites in the rat SOD2 promoter are considered to be GC-rich, this indicates that the SOD2 gene may be a target of promoter methylation where transcription factor binding and therefore transcriptional regulation may become perturbed.

Mechanisms of epigenetic regulation in the SOD2 gene have been demonstrated in a number of disease and natural models (Archer et al., 2010; Hitchler et al., 2006; Hodge et al., 2005; Huang, He & Domann 1999; Thaler et al., 2009). Downregulation of SOD2 has been shown to be mediated by hypermethylation of the SOD2 5' promoter in human multiple myeloma cells (Hodge et al., 2005) and human breast cancer cells (Hitchler et al., 2006) while hypermethylation of the intronic enhancer showed reduced SOD2 expression in SV40-transformed cells (Huang, He & Domann, 1999).

In human multiple myeloma cells hypermethylation was found in a region -191 to 110 of transcription start site, in both AP-2 and Sp1 binding sites. Reversal of this aberrant methylation with the DNA methyltransferase inhibitor Zebularine restored MnSOD gene expression and enzyme levels (Hodge et al., 2005). Similarly, in malignant breast cancer cells analysis of a region -1500 to -1100 in relation to the TSS in the SOD2 promoter demonstrated significantly higher levels of CpG methylation than their normal cell counterparts and lower SOD2 mRNA levels. The causal link between this methylation and SOD2 repression was established when the addition of DNA methyltransferase inhibitor 5-aza-2'-deoxycytidine increased MnSOD mRNA and protein levels (Hitchler et al., 2006). Hypermethylation of the SOD2 intronic enhancer has been demonstrated in pulmonary arterial hypertension (Archer et al., 2010) and in response to diet (Thaler et al. 2009) suggesting that promoter methylation may be a widespread mechanism of SOD2 regulation. It is important to note that binding of transcriptional regulators at the SOD2 gene promoter does not always confer gene activation, therefore the functional significance of promoter hypermethylation is dependent on the biological context within which the affected regions fall.

The two major promoter regions implicated in SOD2 epigenetic regulation are the 5' basal promoter and the intronic enhancer. As discussed, the 5' basal promoter region is rich in binding sites for Sp1 and AP-2 which together seem to constitute the predominant transcription factors regulating SOD2 expression (Xu, Porntadavity & St Clair, 2002). Sp1 is an activating transcription factor that binds directly to DNA and enhances gene transcription (Briggs et al., 1986). It is

essential for both basal and cytokine-induced transcription of SOD2 and requires binding at multiple sites. This allows for the formation of a unique loop structure in the 5' promoter region that is necessary for integrated transcription activation of SOD2 (Mastrangelo et al., 1991). While Sp1 and the elements of the intronic enhancer all appear to have an activating effect on SOD2 transcription, AP-2 has been identified as a SOD2 repressor. AP-2 binds directly to its target gene and is able to facilitate crosstalk between other transcription factors at the gene promoter (Zhu et al., 2001). An immunoprecipitation study and two-hybrid analysis have demonstrated that Sp1 interacts with AP-2 *in vivo* and that this interaction plays both a positive and negative role in gene transcription (Xu, Porntadavity & St Clair, 2002). An interaction between AP-2 and SP1 is also suggested by Sp1 and AP-2's overlapping binding sites (Xu, Porntadavity & St Clair, 2002). A putative AP-1 binding site is also present in the 5' basal promoter. AP-1 modulates signal transduction in cell proliferation and transformation and is also subject to redox regulation (Angel & Karin, 1991). Studies have shown an inverse relationship between the levels of SOD2 and AP-1 in the cell, where MnSOD deficiency enhances AP-1 levels leading to an increase in proliferation and apoptosis (Zhao et al., 2002).

The SOD2 intronic enhancer is composed of binding sites for NFKβ, NF-1 and C/EBP and has been identified as the most crucial element for cytokine-mediated induction of MnSOD expression (Rodgers et al., 2000). A number of studies have established that levels of steady-state MnSOD mRNA and protein increase following exposure to bacterial lipopolysaccharide, tumour necrosis factor and interleukin-1, suggesting that MnSOD plays a critical role in proinflammatory responses (Visner et al., 1990; Visner et al., 1991).

It has been established that the 5' promoter region of the SOD2 gene contains a number of important transcriptional regulatory elements that are GC-rich or contain at least one GC dinucleotide, rendering them susceptible to methylation. It has also been demonstrated that methylation of these regions can lead to SOD2 down-regulation in various biological contexts. However, to date the epigenetic regulation of the rat SOD2 gene has not been investigated in

aging. This study addressed this question by assaying a region of the SOD2 promoter for aberrant methylation using bisulfite conversion and methylation-specific PCR (MS-PCR).

The afore-mentioned methylation assay revealed that the rat SOD2 promoter region approximately -300 bp upstream to 120+ bp downstream of the transcription start site remains largely unmethylated with aging however two aberrantly methylated GC dinucleotide sites were detected. The multiple sequence alignment of each group (young and old) and the unconverted 1A amplicon clearly illustrates that there were no methylated cytosines present in the original amplicons of either groups as 100 % of cytosine residues in both promoter regions have been converted into uracil and subsequently thymine (Figure 17). The multiple sequence alignment of young and old groups and the unconverted 1D amplicon illustrates slightly more variable results (Figure 18). While the majority of CpG dinucleotides contain unmethylated cytosine in both groups, there are two exceptions. In region 1D isolated from young brain tissue (Figure 18 A) 1 cytosine residue appears to be methylated and is located in the 22nd CpG dinucleotide highlighted. This methylation is present in 1 out of 7 amplicons sequenced. In region 1D isolated from old brain tissue (Figure 18 B) 1 cytosine residue appears to be methylated and is located in the 2nd CpG dinucleotide highlighted. This methylation is present in 2 out of 8 amplicons sequenced.

When mapped to the annotated rat SOD2 promoter sequence these cytosines appear at position -40 bp and 85+ bp relative to the TSS. Therefore it can be said that the cytosine at position -40 bp had a methylation frequency of 14.3 % in amplicons derived from young brain tissue and 0 % in amplicons derived from old brain tissue while the cytosine at position 85+ bp had a methylation frequency of 25% in amplicons derived from old brain tissue and 0 % in amplicons derived from young brain tissue.

As stated, the effect cytosine methylation may have on the overall SOD2 gene expression is highly dependent on its regional context. The -40 bp cytosine lies outside of any putative transcriptional binding sites, therefore it would be difficult to speculate as to the biological significance it may

have without further experimental work. However the 85+ bp cytosine is directly adjacent to a Sp1 binding sequence positioned at 78+ bp relative to the TSS (Figure 2). The methylation of this cytosine could therefore confer a biologically significant effect by influencing the binding of Sp1 at this site. In general terms, CpG methylation can sterically hinder potential binding proteins thereby preventing their regulatory control (Holliday, 2006). As Sp1 is an activating transcription factor for SOD2, prevention of its binding would have a negative effect on SOD2 expression. Additionally, the presence of CpG methylation allows a DNA sequence to be targeted by various methyl-binding domain proteins which can go on to recruit and interact with histone deactylases (HDACs) and histone methyltransferases (HMTs). This integrated response to DNA methylation can result in the formation of repressive chromatin structures that ultimately lead to decreased gene expression (Holliday, 2006).

In saying this, gene silencing as a result of DNA methylation is more commonly a result of hypermethylation across the promoter region and not methylation of a single site. Epigenetic downregulation of SOD2 was attributed to CpG hypermethylation detected across eight CpG sites in human breast cancer cells (Hitchler et al., 2006) and across 10 CpG sites in human multiple myeloma cells (Hodge et al., 2005). However, contrary to this, in a study investigating the epigenetic changes in SOD2 in pulmonary arterial hypertension, differential hypermethylation was detected in one CpG site only in the SOD2 intronic enhancer region, and demethylation of this site with 5-AZA treatment increased SOD2 mRNA and protein in a dose-dependent manner (Archer et al., 2010). Therefore it is clear that the effect individual CpG methylation sites may have on overall SOD2 expression is dependent on their location and biological context.

The methylation assay performed for the region -300 bp to 120+ bp of the rat SOD2 promoter only detected 2 differentially methylated sites out of a total of 46 CpG dincleotides present in this region. This suggests that the promoter region remains largely unmethylated with aging. Although the 85+ bp cytosine is located adjacent to a Sp1 binding site, the presence of numerous other unmethylated Sp1 binding sites in the promoter is likely to render the effect of a single methylated cytosine insignificant.

The importance of individual Sp1 binding sites has been assessed in the human SOD2 promoter. Systematic deletion analysis as well as site-specific mutagenesis analysis performed by Xu, Porntadavity & Clair (2002) revealed that a fragment -555 to 24+ bp in the promoter region, containing clusters of Sp1 and AP-2 sites, was sufficient for high-level transcription of the reporter gene. Within this region, at least two binding motifs were needed to achieve minimal transcriptional activity and all binding motifs were required to achieve high levels of transcriptional activity (Xu, Porntadavity & Clair, 2002). Although the rat and human SOD2 promoter regions are not identical in their structure and relative locations of Sp1 binding sites, it is likely that the Sp1 site detected at 78+ bp, adjacent to the 85+ bp differentially methylated cytosine, falls outside of this critical region, as it would on the human gene. Therefore it is unclear whether methylation at this site would confer any significant influence on overall SOD2 expression. However in order to conclusively eliminate epigenetic regulation as an underlying cause for aberrant SOD2 expression and MnSOD activity in aging, further work would need to be undertaken.

This could entail a reproduction of the methylation assay performed in this study, however on a broader scope. This study assessed 2 to 3 clones representing each promoter region (1A and 1D covering a region -300 bp to 120+ bp relative to the TSS) from each rat, where 3 rats were used per age group (young and old). If the sample size and the number of clones per DNA fragment were increased it may be possible to confirm whether the aberrant methylation observed in region 1D originating from old rats has a significant increase in frequency compared to those of young rats or if these observations were simply anomalies.

Additionally, it would be of use to confirm whether methylation in this specific region would have a significant impact on overall SOD2 expression. This could be explored using transfection studies and methylated SOD2-CAT promoter-reporter constructs similar to those used by Huang et al. (1996). This experiment demonstrated that methylation of specific cytosines in the SOD2 5' flanking region is sufficient to repress transcriptional activity of the SOD2 promoter by at least 50

%. Another consideration would be the investigation of methylation content in other significant regulatory regions in the rat SOD2 promoter, such as the intronic enhancer region, that has been shown to be epigenetically regulated in age-related diseases (Huang, He & Domann, 1999; Archer et al., 2010). It is possible that although limited methylation was detected in the SOD2 5' promoter region in this study, age-related methylation may occur in the enhancer region found in intron 2. This would affect the capacity for SOD2 to respond to cytokine-mediated induction of gene expression as opposed to basal levels of gene expression.

8.3. CONCLUSION

MnSOD is a vital antioxidant enzyme that has been shown to decrease in activity with aging. The biological mechanism underlying this down-regulation has not yet been elucidated. An RT-PCR analysis of SOD2 mRNA levels in old rat tissues compared to young rat tissues revealed a subtle increase and decrease of mRNA in old liver and brain tissue respectively, however these results were not proved to be statistically significant. This data may indicate that the reduced activity of MnSOD seen in aging is a result of regulation at a post-transcriptional level or that the subtle changes seen in SOD2 mRNA levels in aging rat tissue may have biological significance, but a larger sample size is required to validate these trends statistically. Based on this assumption and the knowledge that the SOD2 gene is susceptible to epigenetic regulation in various age-related disease models, epigenetic regulation of the SOD2 gene promoter in an age-related context was investigated with a methylation assay. While 2 aberrantly methylated cytosine residues were detected in the rat SOD2 5' promoter region, the majority of the promoter DNA assessed remained unmethylated with aging. This suggests that a reduction in SOD2 levels in aging brain tissue is unlikely to be a result of aberrant epigenetic regulation. In order to further explore epigenetic modification of the SOD2 gene promoter with aging, it may be useful to reproduce the methylation assay performed in this study on a larger scale with regard to the sample size, the number of clones assessed and the regions of the SOD2 promoter investigated.

9. REFERENCES

Alexeyev, M. F., Doux, S.P.L.E. and Wilson, G. L. (2004). Mitochondrial DNA and aging. *Clinical Science,* 364, 355-364.

Angel, P., and Karin, M. (1991). The role of Jun, Fos and the AP-1 complex in cell-proliferation and transformation. *Biochimica Biophysica Acta*, 1072, 129-157.

Aquila, P. D., Rose, G., Bellizzi, D., and Passarino, G. (2012). Epigenetics and Aging. *Maturitas,* 1-7.

Archer, S.L., Marsboom, G., Kim, G.H., Zhang, H.J., Toth, P.T. Svensson, E.C., Dyck, J.R.B., Gomberg-Maitland, M., Thebaud, B., Hsain, A.N., Cipriani, N. and Rehman, J. (2010). Epigenetic attenuation of mitochondrial superoxide dismutase 2 in pulmonary arterial hypertension: a basis for excessive cell proliferation and a new therapeutic target. *Circulation,* 121, 2661-2671.

Balaban, R.S., Nemoto, S. and Finkel. (2005). Mitochondria, oxidants and aging. *Cell*, 120, 483-495.

Barja, G. (2013). Updating the nitochondrial free radical theory of aging: an integrated view, key aspects, and confounding concepts. *Antioxidants & Redox Signalling*, 19(12), 1420-1445.

Bette, M., Schlimme, S., Mutters, R., Menendez, S., Hoffman, S. and Schulz, S. (2004). Influence of different anaesthetics on pro-inflammatory cytokine expression in rat spleen. *Laboratory Animals*, 38, 272-279.

Briggs, M.R., Kadonaga, J.T., Bell, S.P. and Tjian, R. (1986). Purification and biochemical characterization of the promoter-specific transcription factor, Sp1. *Science*, 234, 47-52.

Brown, K., Xie, S., XIAOlei, Q., Mohrin, M., Shin, J., Liu, Y., Zhang, D., Scadden, D.T. and Chen, D. (2013). SIRT3 reverses aging-associated degeneration. *Cell Reports*, 3(2), 319-327.

Bustin, S.A., Benes, V., Garson, J.A., Hellemans, J., Huggett, J., Kubista, M., Mueller, R., Nolan, T., Pfaffl, M.W., Shipley, G.L., Vandesompele, J. and Wittwer, C.T. (2009). The MIQE guidelines: minimum information for publication of quantitative real-time PCR experiments. *Clinical Chemistry*, 55(4), 1-12.

Butterfield, D.A., Castegna, A., Lauderback, C.M. and Drake, J. (2002). Evidence that amyloid beta-peptide-induced lipid peroxidation and its sequelae in Alzheimer's disease brain contribute to neuronal death. *Neurobiology and Aging,* 23, 655-664.

Cand, F. and Verdetti, J. (1989). Superoxide dismutase, glutathione peroxidase, catalase, and lipid peroxidation in the major organs of the aging rats. *Free Radical Biology & Medicine*, 7, 59-63.

Choudhary, C., Kumar, C., Gnad, F., Nielson, M.L., Rehman, M., Walther, T.C., Olsen, J.V. and Mann, M. (2009). Lysine acetylation targets protein complexes and co-regulates major cellular functions. *Science*, 325, 834-840.

Chung, D.J., Wright, A.E. and Clerch, L.B. (1998). The 3' untranslated region of manganese superoxide dismutase RNA contains a translational enhancer element. *Biochemistry*, 37, 16298-16306.

Davis, C.A., Monnier, J.M. and Nick, H.S. (2001). A coding region determinant of instability regulates levels of manganese superoxide dismutase mRNA. *The Journal of Biological Chemistry*, 276, 37317-37326.

DeAngelis, J.S. and Farrington, W.J. (2008). An overview of epigenetic assays. *Molecular Biotechnology*, 38(2), 179-183.

Dioum, E.M., Chen, R., Alexander, M.S., Zhang, Q., Hogg, R.T., Gerard, R.D. and Garda, J.A. (2009). Regulation of hypoxia-inducible factor 2α signaling by the stress-responsive deacetylase sirtuin 1. *Science*, 324, 1289-1293.

Ehrlich, M. (2002). DNA methylation in cancer: too much, but also too little. *Oncogene,* 21, 5400-5413.

Esposito, L., Raber, J., Kekonius, L., Yan, F., Yu, G.-Q., Bien-Ly, N. and Mucke, L. (2006). Reduction in mitochondrial superoxide dismutase modulates Alzheimer's disease-like pathology and accelerates the onset of behavioral changes in human amyloid precursor protein transgenic mice. *The Journal of Neuroscience : The Official Journal of the Society for Neuroscience,* 26(19), 5167-5179.

Flint, D.H. *et al*. (1993). The inactivation of Fe-S cluster containing hydrolases by superoxide. *The Journal of Biological Chemistry,* 268, 22369-22376.

Gentilini, D., Mari, D., Castaldi, D., et al. (2012). Role of epigenetics in human aging and longevity: genome-wide DNA methylation profile in centenarians and centenarians' offspring. *Age,* 35(5), 1961-1973.

Gupta, R.K., Patel, A.K., Shah, N., Chaudhary, A.K., Jha, U.K., Yadav, U.C., Gupta, P.K. and Pakuwal, U. (2014). Oxidative stress and antioxidants in disease and cancer: a review. *Asian Pacific Journal of Cancer Prevention*, 15(11), 4405-4409.

Harman, D. (1957). Ageing: a theory based on free radical and radiation chemistry. *The Journal of Gerontology,* 2, 298-300.

Harman, D. (2006). Free radical theory of aging: an update: increasing the functional life span. *Annals of the New York Academy of Sciences,* 1067, 10-21.

Herman, J.G. and Baylin, S.B. (2003). Gene silencing in cancer in association with promoter hypermethylation. *New England Journal of Medicine,* 349, 2042-2054.
Hitchler, M., Wikainapakul, K., Yu, L. Powers, K., Attatippaholkun, W. and Domann, F.E. (2006). Epigenetic regulation of manganese superoxide dismutase expression in human breast cancer cells. *Epigenetics,* 1(4), 163-171.

Ho, Y.S., Howard, A.J. and Crapo, J.D. (1991). Molecular structure of a functional rat gene for manganese-containing superoxide dismutase. *American Journal of Respiratory Cell and Molecular Biology,* 4, 278-286.

Hodge, D.R., Peng, B., Pompeia, C., Thomas, S., Cho, E., Clausen, P.A., Marquez, V.E. and Farrar, W.L. (2005). Epigenetic silencing of manganese superoxide dismutase (SOD-2) in KAS 6/1 human multiple myeloma cells increases cell proliferation. *Cancer Biology & Therap*y, 4(5), 585-592.

Holliday, R. (2006). Epigenetics: A Historical Overview. *Epigenetics*, 1(2), 76-80.

Hollstein, M., Sidransky, D., Vogelstein, B. and Harris, C.C. (1991). p53 mutations in human cancers. *Science,* 253, 49-53.

Huang, Y., He, T., and Domann, F. E. (1999). Decreased expression of manganese superoxide dismutase in transformed cells is associated with increased cytosine methylation of the SOD2 gene. *DNA and Cell Biology,* 18(8), 643-652.

Huang, Y., Peng, J., Oberley, L.W. and Domann, F.E. (1996). Transcriptional inhibition of manganese superoxide dismutase (SOD2) gene expression by DNA methylation of the 5' CpG island. *Free Radical Biology & Medicine*, 23(2), 314-320.

Huang, T., Yasunami, M., Carlson, E.J., Gillespie, A.M., Reaume, A.G., Hoffman, E.K., Chan, P.H., Scott, R.W. and Epstein, C.J. (1997). Superoxide-mediated cytotoxicity in superoxide dismutase-deficient fetal fibroblasts. *Archives of Biochemistry and Biophysics*, 344(2), 424-432.

Hulbert, A.J., Pamplona, R., Buffenstein, R. and Buttemer, W.A. (2007). Life and Death: Metabolic rate, membrane composition and life span of animals. *Physiological Reviews*, 87(4), 1175-1213.

Illingworth, R.S. and Bird, A.P. (2009). CpG islands–'a rough guide.' *FEBS Letters*, 583, 1713-1720.

Ischiropoulos, H. and Beckman, J. S. (2003). Oxidative stress and nitration in neurodegeneration : Cause, effect, or association? *Neurodegeneration,* 111(2), 163-169.

Jones, P.L., Kucera, G., Gordon, H. and Boss, J.M. (1995). Cloning and characterization of the murine manganous superoxide dismutase-encoding gene. *Gene,* 153, 155-161.

Jones, P.A. and Baylin, S.B. (2007). The Epigenomics of Cancer. *Cell,* 128, 683-692.

Jintaridth, P. and Mutirangura, A. (2010). Distinctive patterns of age-dependent hypomethylation in interspersed repetitive sequences. *Physiological Genomics*, 41, 194-200.

Keller, J. N., Kindy, M. S., Holtsberg, F. W., Clair, D. K. S., Yen, H., Germeyer, A. and Mattson, M. P. (1998). Apoptosis and Reduces Ischemic Brain Injury: Suppression of Peroxynitrite Production, Lipid Peroxidation, and Mitochondrial Dysfunction. *The Journal of Neuroscience : The Official Journal of the Society for Neuroscience,* 18(2), 687-697.

Kim, S.C., Sprung, R., Chen, Y., Xu, Y., Ball, H., Pei, J., Cheng, T., Kho, Y., Xiao, L., Grishin, N.V., White, M., Yang, X.J. and Zhao, Y. (2006). Substrate and functional diversity of lysine acetylation revealed by a proteomics survey. *Molecular cell*, 23, 607-618.

Kirkinezos, I. G. and Moraes, C. T. (2001). Reactive oxygen species and mitochondrial diseases. *Seminars in Cell & Developmental Biology,* 12(6), 449-457.

Klose, R.J. and Bird, A.P. (2006). Genomic DNA methylation: the mark and its mediators. *Trends in Biochemical Sciences,* 31, 89-97.

Knirsch, L. and Clerch, L.B. (2000). A region in the 3' UTR of MnSOD RNA enhances translation of a heterologous RNA. *Biochemical and Biophysical Research Communications*, 272, 164-168.

Kuo, S., Chesrown, S. E., Mellott, J.K., Rodgers, R.J., Hsu, J. and Nick, H.S. (1999). *In vivo* architecture of the manganese superoxide dismutase promoter. *The Journal of Biological Chemistry*, 274(6), 3345-3354.

Kokoszka, J.E., Coskun, P., Esposito, L.A. and Wallace, D.C. (2000). Increased mitochondrial oxidative stress in the Sod2 (+/-) mouse results in the age-related decline of mitochondrial function culminating in increased apoptosis. *PNAS*, 98(5), 2278-2283.

Lee, J., Koo, N., & Min, D. B. (2004). Species, Aging, and Antioxidative Nutraceuticals. *Comprehensive Reviews in Food Science and Food Safety,* 3*,* 21-33.

Liochev, S.I. (2013). Reactive oxygen species and the free radical theory of aging. *Free Radical Biology and Medicine*, 60, 1-4.

Lin, S., Kaeberlein, M., Andalis, A.A., Sturtz, L.A., Defossez, P., Culotta, V.C., Fink, G.R. and Guarente, L. (2002). Clorie restriction extends *Saccharomyces cerevisiae* life span by increasing respiration. *Nature*, 418, 344-348.

Loft, S. and Poulsen, H.E. (1996). Cancer risk and oxidative DNA damage in man. *Journal of Molecular Medicine,* 74, 297-312.

Loo, B., Labugger, R., Skepper, J.N., Bachschmid, M., Kilo, J., Powell, J.M., Palacious-Callender, M., Erusalimsky, J.D., Quaschning, T., Malinski, T., Gygi, D., Ulrich, V and Luscher, T.F. (2000). Enhanced peroxynitrate formation is associated with vascular aging. *Journal of Experimental medicine*, 192(12), 1731-1743.

Marcus, D. L., Thomas, C., Rodriguez, C., Simberkoff, K., Tsai, J. S., Strafaci, J.A. and Freedman, M. L. (1998). Increased peroxidation and reduced antioxidant enzyme activity in Alzheimer's disease. *Experimental Neurology,* 150(1), 40-44.

Martin, R., Fitzl, G., Mozet, C., Martin, H., Welt, K. and Wieland, E. (2002). Effect of age and hypoxia/reoxygenation on mRNA expression of antioxidant enzymes in rat liver and kidneys. *Experimental Gerontology*, 37, 1479-1485.

Mastrangelo, I.A., Courey, A.J., Wall, J.S., Jackson, S.P. and Hough, P.V. (1991). DNA looping and Sp1 multimer links: a mechanism for transcriptional synergism and enhancement. *PNAS USA*, 88, 5670-5674.

Matés, J. M. (2000). Effects of antioxidant enzymes in the molecular control of reactive oxygen species toxicology. *Toxicology,* 153(1-3), 83-104.

Matés, J. M., Segura, J.A., Alonso, F.J., Márquez, J. (2012). Oxidative stress in apoptosis and cancer: an update. *Archives of Toxicology*, 86(11), 1649-1665.

Miao, L. and Clair, D. S. (2009). Regulation of superoxide dismutase genes: implications in disease. *Free Radical Biology and Medicine,* 47(4), 344-356.

Navarro, A. and Boveris, A. (2004). Rat brain and liver mitochondria develop oxidative and lose enzymatic activities on aging. *The American Journal of Physiology. Regulatory, Integrative and Comparative Physiology,* 287, R1244-R1249.

Navarro, A., Gomez, C., Lopez-Cepero, J.M. and Boveris, A. (2003). Beneficial effects of moderate exercise on mice aging: survival, behavior, oxidative stress, and mitochondrial

electron transfer. *The American Journal of Physiology. Regulatory, Integrative and Comparative Physiology*, 286, R505-R511.

Ozden, O., Park, S., Kim, H. Jiang, H., Coleman, M.C., Spitz, D.R. and Gius, D. (2011). Acetylation of MnSOD directs enzymatic activity responding to cellular status or oxidative stress. *Aging*, 3(2), 102-107.

Rai, P. and Troen, B.R. (2011). Cell and molecular aging. *Principles and Practice of Geriatric Surgery*, 5-37.

Rao, G., Xia, E. and Richardson, A. (1990). Effect of age on the expression of antioxidant enzymes in male Fischer F344 rats. *Mechanisms of Ageing and Development*, 53, 49-60.

Rattan, S. I. S. (2006). Theories of biological aging: genes, proteins, and free radicals. *Free Radical Research,* 40(12), 1230-1238.

Reddy, P. (2009). The role of mitochondria in neurodegenerative diseases: mitochondria as a therapeutic target in Alzheimer's disease. *CNS Spectrums,* 14, 8-18.

Richardson, B. (2003). Impact of aging on DNA methylation. *Ageing Research Reviews,* 2, 194-200.

Rodgers, R.J., Chesrown, S.E., Kuo, S., Monnier, J.M. and Nick, H.S. (2000). Cytokine-inducible enhancer with promoter activity in both the rat and human manganese-superoxide dismutase genes. *Biochemistry Journal,* 347, 233-242.

Rosen, D.R., Siddique, T., Patterson, D., et al (1993). Mutations in Cu/Zn superoxide dismutase gene are associated with familial amyotrophic lateral sclerosis. *Nature*, 362, 59-62.

Soo You, J., Jones, P.A. (2012). Cancer genetics and epigenetics: Two sides of the same coin? *Cancer Cell*, 22(1), 9-20.

Smalheiser, N.R. and Torvik, V.I. (2006). Alu elements within human mRNAs are probable microRNA targets. *Trends in Genetics*, 22, 532-536.

Stuart, J.J., Egry, L.A., Wong, G.H. and Kaspar, R.L. (2000). The 3' UTR of human MnSOD mRNA hybridizes to a small cytoplasmic RNA and inhibits gene expression. *Biochemical and Biophysical Research Communications*, 274, 641-648.

Sutherland, G.T., Chami, B., Youssef, P. and Witting, P.K. (2013). Oxidative stress in Alzheimer's disease: Primary villain or physiological by-product? *Redox Report*, 18(4), 134-141.

Taby, R. and Issa, J.J. (2010). Cancer Epigenetics. *CA: A Cancer Journal for Clinicians,* 60, 376-392.

Tao, R., Coleman, M.C., Pennington, D., Ozden, O., Park, S., Jiang, H., Kim, H., Flynn, C., Hill, S., McDonald, W.H., Olivier, A.K. and Spitz, D.R. (2010). Sirt3-mediated deactylation of evolutionarily conserved lysine 122 regulates MnSOD activity in response to stress. *Molecular Cell*, 40, 893-904.

Thaler, R., Karlic, H., Rust, P. and Haslberger, A.G. (2008). Epigenetic regulation of human buccal mucosa mitochondrial superoxide dismutase gene expression by diet. *British Journal of Nutrition*, 101, 743-749.

Tian, L., Cai, Q. and Wei, H. (1998). Alterations of antioxidant enzymes and oxidative damage to macromolecules in different organs of rats during aging. *Free Radical Biology & Medicine*, 24(9), 1477-1484.

Toyota, M., & Issa, J. P. (1999). CpG island methylator phenotypes in aging and cancer. *Seminars in Cancer Biology,* 9(5), 349-357.

Tsai, H. and Baylin, S.B. (2011). Cancer epigenetics: linking basic biology to clinical medicine. *Cell Research,* 21, 502-517.

Tsay, H., Wang, P., Wang, S. and Ku, H. Age-associated changes of superoxide dismutase and catalase activities in the rat brain. *Journal of Biomedical Sciences*, 7, 466-474.

Valko, M., Leibfritz, D., Moncol, J., Cronin, M. T. D., Mazur, M., & Telser, J. (2007). Free radicals and antioxidants in normal physiological functions and human disease. *The International Journal of Biochemistry & Cell Biology,* 39(1), 44-84.

Velarde, M.C., Flynn, J.M., Day, N.U., Melov, S. and Campisi, J. (2012). Mitochondrial oxidative stress caused by Sod2 deficiency promotes cellular senescence and aging phenotypes in the skin. *Aging*, 4(1), 3-12.

Visner, G.A., Block, E.R., Burr, I.A. and Nick, H.S. (1991). Regulation of manganese superoxide dismutase in porcine pulmonary artery endothelial cells. *American Journal of Physiology*, 260(6), L444-L449.

Visner, G.A., Dougall, W.C., Wilson, J.M., Burr, I.A. and Nick, H.S. (1990). Regulation of manganese superoxide dismutase by lipopolysaccharide, Interleukin-1 and Tumour Necrosis Factor. *The Journal of Biological Chemistry*, 265(5), 2856-2864.

Vlaming, H. and van Leeuwen, F. (2012). Crosstalk between aging and the epigenome. *Epigenomics,* 4, 5-7.

Waki, T., Tamura, G., Sato, M., & Motoyama, T. (2003). Age-related methylation of tumor suppressor and tumor-related genes: an analysis of autopsy samples. *Oncogene,* 22(26), 4128-4133.

Wan, X.S., Devalaraja, M.N. and St Clair, D.K. (1994). Molecular structure and organization of the human manganese superoxide dismutase gene. *DNA and Cell Biology,* 13, 1127 – 1136.

Wang, S.C., Oelze, B. and Schumacher, (2008). Age-specific epigenetic drift in late-onset Alzheimer's disease. *PLoS ONE,* 3, 2698-2871.

Waris, G. and Ahsan, H. (2006). Reactive oxygen species: role in the development of cancer and various chronic conditions. *Journal of Carcinogenesis,* 5, 14-21.

Warner, H.R. (1994). Superoxide dismutase, aging and degenerative disease. *Free Radical Biology and Medicine*, 17(3), 249-258.

Wickens, A. P. (2001). Ageing and the free radical theory. *Respiration Physiology,* 128, 379-391.

Winnefeld, M. and Lyko, S. (2012). The aging epigenome: DNA methylation from the cradle to the grave. *Genome Biology,* 13, 156.

Wood, J.G., Rogina, B., Lavu, S., Howitz, K., Helfand, S.L., Tatar, M. and Sinclair, D. (2004). Sirtuin activators mimic caloric restriction and delay ageing in metazoans. *Nature*, 430, 686-689.

Xu, S., Ying, J., Jlang, B., Guo, W., Adachi, T., Sharov, V., Lazar, H., Menzolan, J., Knyushko, V., Bigelow, D., Schonelch, C. and Cohen, R.A. (2006). Detection of sequence-specific tyrosine nitration of manganese SOD and SERCA in cardiovascular disease and aging. *American Journal of Physiology*, 290, H2220-H2227.

Xu, Y., Porntadavity, S. and St Clair, D.K. (2002). Transcriptional regulation of the human manganese superoxide dismutase gene: the role of specificity protein 1 (Sp1) and activating protein-2 (AP-2). *Biochemistry Journal,* 362, 401-412.

Yen, T., King, K., Lee, H., Yeh, S. and Wei, Y. (1994). Age-dependent increase of mitochondrial DNA deletions together with lipid peroxides and superoxide dismutase in human liver mitochondria. *Free Radical Biology & Medicine*, 16(2), 207-214.

Zawia, N., Lahiri, D. and Cardozo-Pelaez, F. (2009). Epigenetics, oxidative stress, and Alzheimer disease. *Free Radical Biology,* 46(9), 1241-1249.

Zhao, Y., Oberley, T.D., Chaiswing, L., Lin, S.M., Epstein, C.J., Huang, T.T. and St. Clair, D. (2002). Manganese superoxide dismutase deficiency enhances cell turnover via tumor promoter-

induced atlerations in AP-1 and p53-mediated pathways in a skin cancer model. *Oncogene*, 21, 3836-3846.

Zhu, C., Huang, Y., Oberley, L.W. and Domann, F.E. (2001). A family of AP-2 proteins down-regulate manganese superoxide dismutase expression. *The Journal of Biological Chemistry*, 276(17), 14407-14413.

10. APPENDICES

10.1. Appendix A

All agarose gel used in gel electrophoresis was prepared as follows:

5 g Agarose gel

50 ml distilled water

5 µl GRGreen nucleic acid stain

10.2. Appendix B

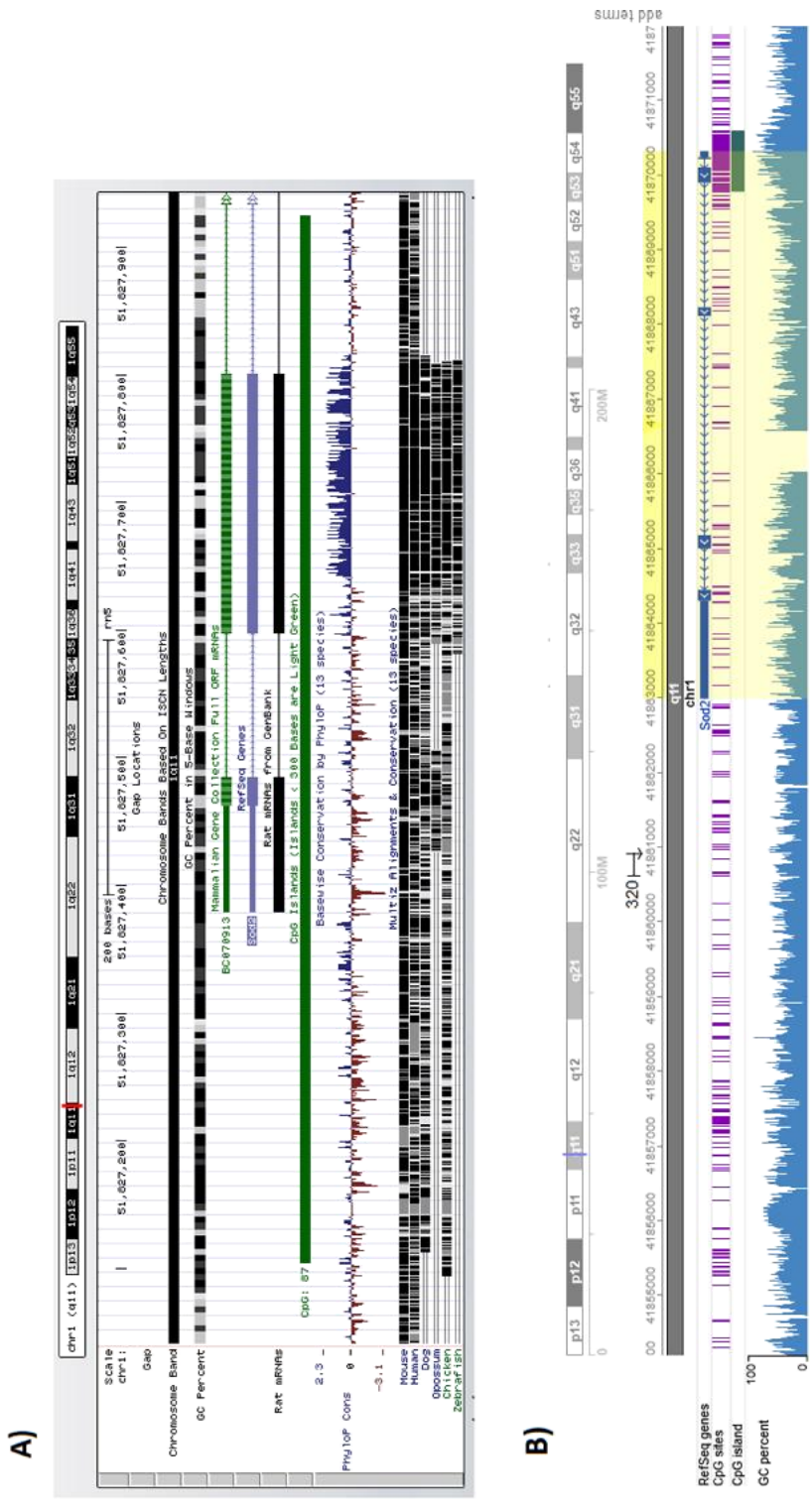


Figure A1. Rat SOD2 promoter annotation illustrating species conservation and GC frequency. A) A region of the rat SOD2 gene as illustrated by the UCSC Genome Browser. The image depicts the gene CpG island shown as a green band, as well as exon 1 and 2. Other features illustrated are the high GC content and the high sequence conservation across 5 species. B) The complete rat SOD2 gene as illustrated by the WashU EpiGenome Browser. The gene is shown in the 3' to 5' direction. The CpG is shown as a green band, exons are shown as blue bands.

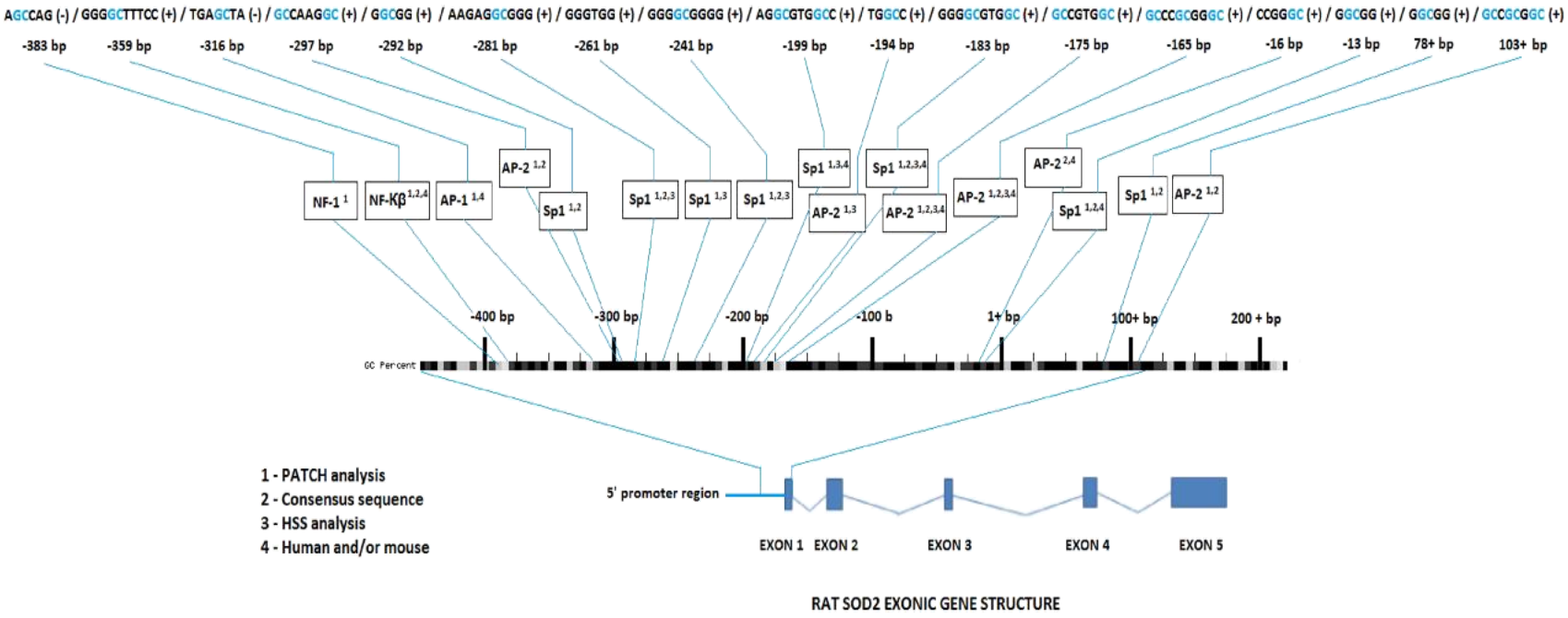


Figure 2. Comprehensive putative annotation of the rat SOD2 gene promoter region. Each annotation is based on more than one source, as indicated by the key. The figure illustrates a region of the 5' promoter and the putative binding sites located within it. The sequence of each binding site and its location are shown in relation to the transcription start site, 1+. The GC dinucleotides in each sequence are shown in blue font. Binding sites for NF-1, NFKβ and AP-1 are located -400 to -300 bp of the TSS, while multiple binding sites for AP-2 and Sp1 are distributed between -300 and 100+ bp of the TSS.

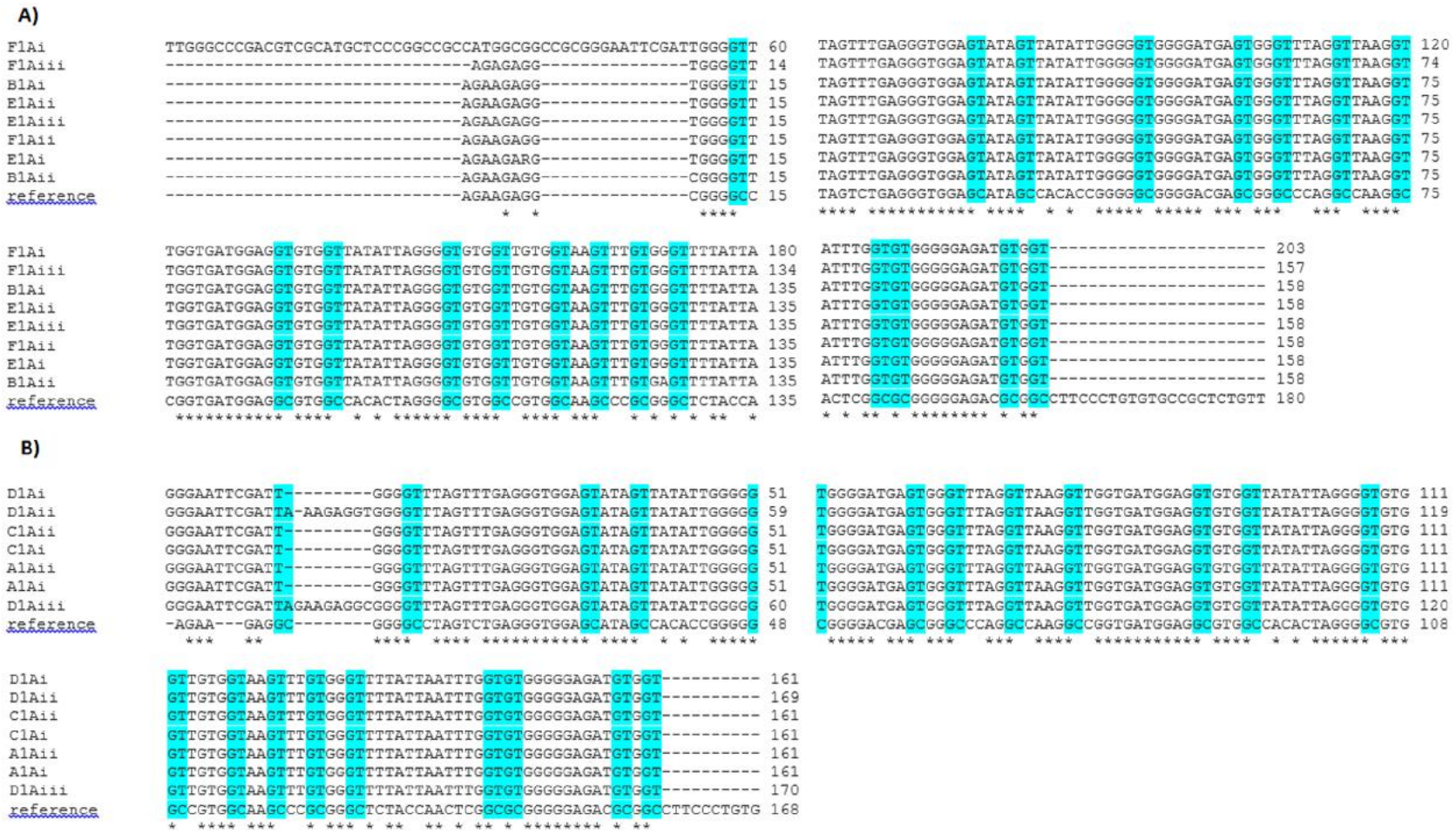


Figure A3. Multiple sequence alignment of rat SOD2 promoter region 1A amplicons derived from brain tissue and the original unconverted DNA sequence. Converted CpG dinucleotides are highlighted in blue. A) All sequences originate from young brain tissue. B) All sequences originate from old brain tissue.

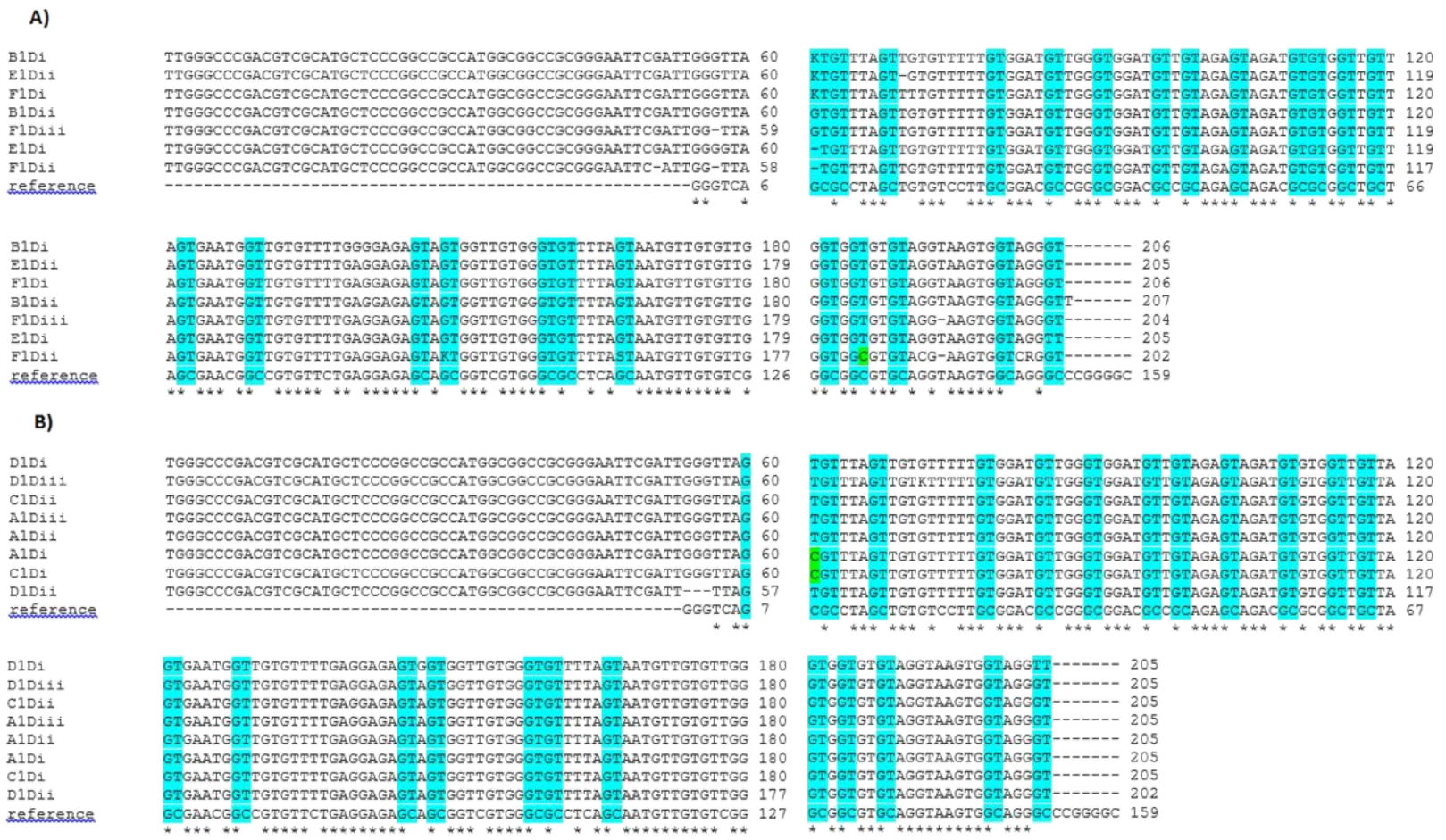


Figure A4. Multiple sequence alignment of rat SOD2 promoter region 1D amplicons derived from brain tissue and the original unconverted DNA sequence. Converted CpG dinucleotides are highlighted in blue, methylated cytosines are highlighted in green. A) All sequences originate from young brain tissue. B) All sequences originate from old brain tissue.

10.3. Appendix C

Table B1. CP data values used to generate standard curves.

SOD2	2.00	1.00	0.00	-1.00	-2.00
	20.23	23.12	27.24	29.52	35.00
	20.43	24.01	27.05	30.60	33.54
	20.46	24.12	26.58	30.60	35.00
Mean	20.37	23.75	26.96	30.24	34.51
SD	0.10	0.45	0.28	0.51	0.69
SE	0.06	0.26	0.16	0.29	0.40
CCT4	2.00	1.00	0.00	-1.00	-2.00
	21.50	24.49	29.31	32.08	35.00
	21.10	24.58	27.14	32.25	35.00
	21.56	25.24	27.45	33.43	35.00
Mean	21.39	24.77	27.97	32.59	35.00
SD	0.20	0.33	0.96	0.60	0.00
SE	0.12	0.19	0.55	0.35	0.00
RAB1	2.00	1.00	0.00	-1.00	
	26.48	29.59	32.30	35.00	
	26.78	29.73	33.19	35.00	
	24.68	28.20	33.14	35.00	
Mean	25.98	29.17	32.88	35.00	
SD	0.93	0.69	0.41	0.00	
SE	0.54	0.40	0.24	0.00	
RPN1	2.00	1.00	0.00	-1.00	-2.00
	21.86	25.05	28.00	33.41	35.00
	22.47	25.66	29.72	33.18	35.00
	21.83	25.78	29.55	33.86	35.00
Mean	22.05	25.50	29.09	33.48	35.00
SD	0.29	0.32	0.77	0.28	0.00
SE	0.17	0.18	0.45	0.16	0.00

Table B2. Raw data readings obtained from RT-PCR using liver tissue.

Liver		RAT A	RAT C	RAT D	RAT B	RAT E	RAT F
SOD2	1	20.21	22.70	22.03	20.30	21.88	21.00
	2	19.83	22.92	21.27	20.23	21.32	21.16
	3	19.83	22.91	21.65	20.43	21.80	21.27
	Mean	19.96	22.84	21.65	20.32	21.67	21.14
	SD	0.18	0.10	0.31	0.08	0.25	0.11
	SE	0.10	0.06	0.18	0.05	0.14	0.06
	NRTC	0.00	0.00	33.30	0.00	0.00	30.74
	NTC	0.00	0.00	31.99	35.00	34.50	35.00
CCT4	1	21.13	24.53	22.04	21.15	21.88	21.96
	2	21.77	24.30	22.06	21.10	21.62	21.96
	3	21.90	24.52	22.10	21.56	21.91	21.90
	Mean	21.60	24.45	22.07	21.27	21.80	21.94
	SD	0.34	0.11	0.02	0.21	0.13	0.03
	SE	0.19	0.06	0.01	0.12	0.08	0.02
	NRTC	0.00	32.36	33.32	0.00	35.00	35.00
	NTC	0.00	32.79	0.00	0.00	35.00	35.00
RAB11B	1	24.25	23.10	25.73	24.31	24.63	23.77
	2	24.34	23.08	25.81	24.47	24.94	23.76
	3	24.29	23.23	25.90	24.95	24.82	23.80
	Mean	24.29	23.14	25.81	24.58	24.80	23.78
	SD	0.04	0.07	0.07	0.27	0.13	0.02
	SE	0.02	0.04	0.04	0.16	0.07	0.01
	NRTC	0.00	31.73	33.18	0.00	32.15	33.17
	NTC	0.00	32.30	0.00	0.00	35.00	0.00
RPN1	1	22.74	21.92	23.35	22.60	22.67	22.23
	2	22.52	21.63	23.26	22.32	22.52	22.36
	3	22.62	22.09	23.44	22.45	22.87	22.32
	Mean	22.63	21.88	23.35	22.46	22.69	22.30
	SD	0.09	0.19	0.07	0.11	0.14	0.05
	SE	0.01	0.03	0.01	0.02	0.02	0.01
	NRTC	0.00	0.00	35.00	0.00	35.00	0.00
	NTC	0.00	0.00	35.00	0.00	35.00	0.00
	Normalised ratio	2.464316	0.452794	1.500661	1.842415	0.628313	1

Table B3. Raw data readings obtained from RT-PCR using brain tissue.

Brain		RAT A 1	RAT C 1	RAT C 2	RAT C 3	RAT D 1	RAT D 2	RAT B 1	RAT B 2	RATE 1	RAT E 2	RAT F 1	RAT F 2
SOD2	1	22.21	20.88	26.77	28.61	21.92	22.77	21.11	24.26	21.82	23.71	21.61	22.54
	2	22.17	21.06	26.97	28.43	21.81	22.77	21.46	23.96	21.76	23.91	21.98	22.59
	3	22.12	21.29	26.67	28.46	21.63	22.63	21.60	23.90	21.93	22.84	21.78	22.26
	Mean	22.17	21.08	26.80	28.50	21.79	22.72	21.39	24.04	21.84	23.49	21.79	22.46
	SD	0.04	0.17	0.12	0.08	0.12	0.07	0.21	0.16	0.07	0.46	0.15	0.15
	SE	0.02	0.10	0.07	0.05	0.07	0.04	0.12	0.09	0.04	0.27	0.09	0.08
	NRTC	0.00	0.00	0.00	0.00	0.00	0.00	0.00	31.65	0.00	26.17	30.01	0.00
	NTC	0.00	0.00	0.00	0.00	0.00	0.00	35.00	0.00	32.70	0.00	0.00	0.00
CCT4	1	22.58	22.51	25.57	27.83	22.56	22.79	21.58	21.43	21.86	23.80	22.08	20.70
	2	21.81	22.60	25.77	27.49	22.75	22.87	21.02	21.25	21.64	23.82	22.45	20.79
	3	21.77	22.75	25.84	27.49	22.75	22.66	20.53	21.79	22.20	23.49	22.23	20.85
	Mean	22.05	22.62	25.73	27.60	22.69	22.77	21.04	21.49	21.90	23.70	22.25	20.78
	SD	0.37	0.10	0.11	0.16	0.09	0.09	0.43	0.22	0.23	0.15	0.15	0.06
	SE	0.22	0.06	0.07	0.09	0.05	0.05	0.25	0.13	0.13	0.09	0.09	0.04
	NRTC	35.00	0.00	0.00	35.00	33.83	35.00	0.00	35.00	0.00	35.00	35.00	35.00
	NTC	0.00	0.00	0.00	0.00	33.12	0.00	0.00	35.00	31.38	0.00	32.03	0.00
RAB11B	1	24.08	20.82	28.90	29.47	22.70	23.31	22.59	26.32	22.80	23.51	22.77	24.53
	2	23.74	20.96	28.55	29.08	22.71	22.97	22.70	26.75	22.63	23.22	22.77	24.23
	3	23.82	20.80	28.65	29.28	22.86	22.99	23.89	26.22	22.70	23.26	22.83	24.29
	Mean	23.88	20.86	28.70	29.28	22.76	23.09	23.06	26.43	22.71	23.33	22.79	24.35
	SD	0.15	0.07	0.15	0.16	0.07	0.16	0.59	0.23	0.07	0.13	0.03	0.13
	SE	0.08	0.04	0.08	0.09	0.04	0.09	0.34	0.13	0.04	0.07	0.02	0.07
	NRTC	35.00	29.31	30.73	0.00	33.53	32.29	35.00	35.00	31.01	32.05	32.23	0.00
	NTC	0.00	0.00	35.00	0.00	0.00	0.00	0.00	0.00	35.00	0.00	35.00	0.00
RPN1	1	25.19	22.52	28.48	29.92	23.59	23.87	22.72	28.03	22.68	23.97	22.89	25.47
	2	23.76	22.11	29.12	30.53	23.59	24.00	22.71	28.33	22.64	23.91	22.96	24.91
	3	24.29	22.17	28.88	30.30	23.63	23.83	23.22	28.04	22.80	24.47	23.25	25.00
	Mean	24.41	22.27	28.83	30.25	23.60	23.90	22.88	28.13	22.71	24.12	23.03	25.13
	SD	0.59	0.18	0.26	0.25	0.02	0.07	0.24	0.14	0.07	0.25	0.16	0.25
	SE	0.08	0.02	0.04	0.03	0.00	0.01	0.03	0.02	0.01	0.03	0.02	0.03
	NRTC	35.00	35.00	35.00	0.00	35.00	0.00	0.00	0.00	35.00	0.00	0.00	35.00
	NTC	0.00	35.00	35.00	0.00	35.00	35.00	35.00	35.00	35.00	0.00	0.00	0.00